UNIVERSITY OF TWENTE

Modelling the impact of storm-induced barrier island breaching on the morphodynamic evolution and stability of multiple tidal inlet systems

Author:
Tessa Andringa

24th November 2017

UNIVERSITY OF TWENTE

MASTER'S THESIS
in Water Engineering and Management
Faculty of Engineering Technology

Modelling the impact of storm-induced barrier island breaching on the morphodynamic evolution and stability of multiple tidal inlet systems

Author	T.E. Andringa BSc tessa_andringa@hotmail.com
Location and date	Enschede, 24th November 2017
Graduation committee	
Graduation supervisor	Prof. dr. S.J.M.H. Hulscher
Daily supervisors	Dr. ir. P.C. Roos Ir. K.R.G. Reef
External supervisor	Dr. ir. A. Dastgheib

Abstract

Barrier island systems occur all over the world and are important in defending the mainland. Next, they are connected to human activities such as navigation, industry and recreation. This makes it important to gain knowledge of the processes and the morphodynamic behaviour of these systems. The tidal inlets separate the barrier islands from each other. Water flows to and from the basin through these inlets because of the tides. As a result, sediment is transported out of the inlets. Waves, on the other hand, cause a longshore sediment transport that results in a sediment import to the inlets. The interplay between waves and tides thus determines the change in inlet morphology.

There is still little knowledge on the long term morphodynamics of tidal inlet systems and their response to external changes. With an idealized model, Roos et al. (2013) demonstrated the existence of multiple stable inlets by accounting for spatially varying water levels. Here, we extend this by including storm-induced inlet formation to identify the evolution of new inlets and their effect on the equilibria of the system.

The first part of the study contains a review of storm-induced barrier island breaching and a historical overview of breach events. The impact of a storm on barrier islands and the occurrence of breaches depend on both hydrodynamical and morphological properties of the environment. Overtopping water can carve channels on the island which can cause a breach. Many of these breach events have been documented in the past, but little data of the breaches and associated storms are available. Analysis of observations show that breaches occur during storms with at least Beaufort Force 10 and that the breach area ranges between roughly 50 and 510 m^2.

The second part of the study contains the long-term modelling of tidal inlet systems and storm-induced breaches. Three probability distributions are implemented in the model to describe breach occurrence and the location and size of the breach. Because of the stochastic forcing, a Monte Carlo analysis is used which produces statistic details of the system's response to the storm-induced breaches.

We start the simulation with one inlet at a random location in the system. Every time step there is the possibility that a breach occurs and a new inlet is created. The cross-sectional area of all inlets change in time until the system reaches its equilibrium state with equilibrium value of total inlet area. Breaches can either close within several years or grow in size which causes existing inlets to decrease in size to restore the equilibrium state. The initial evolution of individual new inlets depends on three factors: proximity to equilibrium, distance to neighbouring inlets and breach size. The lifetime of inlets is higher for inlets further away from existing inlets and with higher initial widths.

This generic model study gives insight in the qualitative evolution of breaches and the interaction among inlets. It helps policy makers showing the possible consequences of a breach. Further research is recommended to reduce the uncertainties and improve (quantitative) precision of the simulation.

Preface

This document is the report of my MSc thesis which is the last part of my study of Water Engineering and Management at the University of Twente. I enjoyed my study in Enschede and learned a lot the last few years. I think I have combined all I learned in this research and I wish you much pleasure reading this report. Though it is an important topic, especially nowadays with challenges as sea level rise, only few is known about the long-term behaviour of tidal inlet systems. I liked to dive into this broad and interesting subject and I hope my results contribute to the knowledge of or interest in tidal inlet systems.

I would like to thank the people who helped me performing this research and guided me trough the graduation process. First of all thanks to my supervisors Suzanne Hulscher, Pieter Roos, Koen Reef and Ali Dastgheib. I received critical but helpful feedback from all of you. From each person from a different point of view what really improved my thesis. Sometimes the number of comments were a lot, but the smileys that were drawn next to them by Pieter always encouraged me to work further.

Besides, I would like to thank my friends for the nice walks and talks when I needed distraction, my parents for having faith in me and encouraging me to go study, Esther for always being there and Sander for all his help and cheering up the past half year.

Tessa Andringa,
Enschede, November 2017

Contents

Chapter 1

Introduction

1.1 Background

1.1.1 Barrier coast systems

Around 10 percent of the worlds open coasts are barrier coasts, formed a long time ago as a result of sea level rise (Stutz and Pilkey, 2011). Islands occur all over the world but mostly in areas with a low gradient in the slope of the shore and tectonically inactive zones. A barrier coast consists of six elements: mainland (or coast), backbarrier lagoon (or basin), inlet and inlet deltas, barrier islands, barrier platform and shoreface (shore zone of the sea floor) (Oertel, 1985). The inlets separate barrier islands and connect the basin to the sea, so water and sediment can be transported from and to the basin. The geometry and processes in and near these inlets constitute the tidal inlet system. The geomorphology and processes of the tidal inlet system are shown in Figure 1.1.

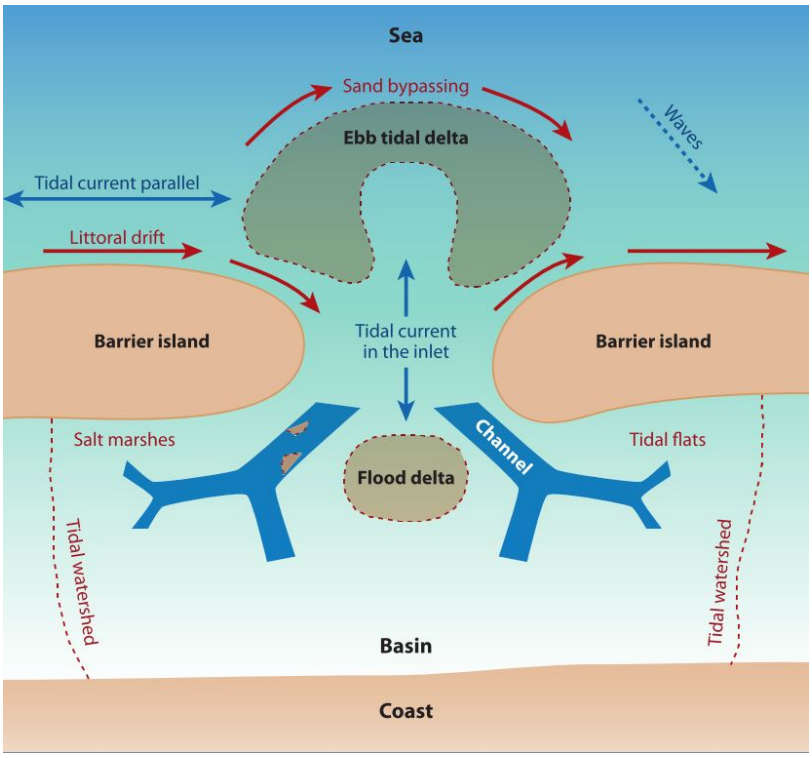

FIGURE 1.1: Processes and geomorphology of tidal inlet system - (De Swart and Zimmerman, 2009). Showing coast, basin, inlet and inlet deltas, barrier islands and sea

Barrier coasts differ in geometry and can be classified based on geology, climate and the wave tide regime of the area (Stutz and Pilkey, 2011). Barrier islands vary in length between 1 and 50 kilometres whereas the cross sectional area of inlets varies between 10^3 and 10^5 m^2 (De Swart and Zimmerman, 2009). The cross sectional area of inlets is related to the tidal prism: the volume of water flowing through the inlet between high and low tide (Tran et al., 2012). Larger basins attract more water and thus let the inlets deal with a greater tidal prism (Oertel, 1985).

The evolution of the tidal inlet system can be described by the morphological loop as shown in Figure 1.2. Hydrodynamics affect sediment transport which causes morphological changes. The hydrodynamics will respond to these changes which closes the loop. In hydrodynamics we distinguish waves and tides. In mesotidal coasts, waves and tides are of equally importance and the competing effects of these two groups determine the morphological evolution of barrier coasts (De Swart and Zimmerman, 2009). Waves in the sea often approach the shore in an oblique angle which leads to a longshore current along the seaward side of the barrier islands. Part of this sediment will reach the tidal inlet where it will be deposited. Waves thus cause a sediment import. Tides on the other hand cause a sediment flux out of the inlet. Tidal currents move through the inlet towards the basin during flood and back during ebb. These tidal currents cause a net export of sediment out of the inlet. The interaction between the wave and tide processes define the geometry of the inlets. An increasing importance of waves relative to tides leads to filling of the inlets and thus fewer and narrower inlets (Hayes, 1979).

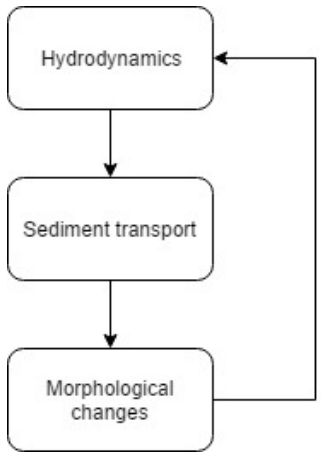

FIGURE 1.2: Morphological loop

Knowledge of long-term behaviour of barrier island systems is important because the system facilitates lots of functions. Primarily, the islands form a coastal defence for habitants of the mainland. In addition, humans use the island for various activities: industry, agriculture, recreation and navigation (Stutz and Pilkey, 2005). To support these functions, the barrier coast systems have to be maintained. This is not possible without knowledge of the morphodynamic behaviour and the processes affecting this morphodynamic behaviour. Today's challenges as sea level rise and climate change (inducing change in storm severity and frequency) and also human interventions affect these barrier coastal systems even more. This enlarges the need to gain understanding of the system.

1.1.2 Storm-induced formation of tidal inlets

Storms influence coastal systems and especially vulnerable to storms are barrier coasts (Wang and Roberts Briggs, 2015). Depending on hydrodynamic properties (such as duration and elevation of the surge and wave height and period) and on the morphological properties of the system (such as height and width of the island and dunes), a storm event can cause a barrier island to breach.

The initial state of inlet formation process is crucial to permanent inlet formation (Friedrichs et al., 1993) and the breach channels widen and deepen quickly (Kraus et al., 2002). The newly formed inlet may change the hydrodynamics of other inlets, for example the tidal prism of existing inlets might decrease as in the study of Wang and Beck (2012). As pointed out in section 1.1.3, a change in the hydrodynamics causes

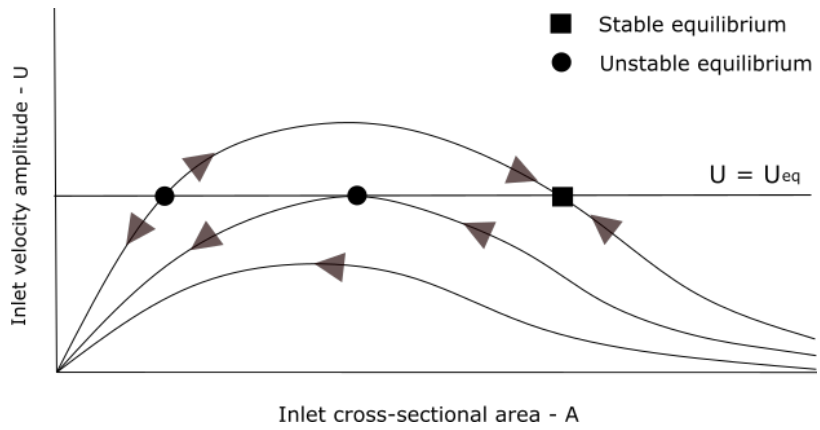

FIGURE 1.3: Closure curves of Escoffier (1940) showing inlet velocity (U) and equilibrium inlet velocity (U_eq) as a function of inlet cross sectional area (A). Intersections show equilibria of the inlet and the arrows indicate the tendency of the system in time.

changes in the morphology. These new inlets thus compete with the old inlets which can result in closure of one or more of these inlets. Knowledge of the behaviour of tidal inlets systems is still lacking. But the tendency of an inlet to stay open or to close can be studied using the stability concept of Escoffier (1940). Changes in morphology continue until there is a balance between sediment import and export so an equilibrium state is reached. The equilibrium state can be either stable or unstable. An inlet is in stable equilibrium when after a perturbation the inlet returns to its previous (equilibrium) state. So in a stable equilibrium, a perturbation affecting the geometry or velocity in the inlet results in forces that tend to restore the equilibrium state.

1.1.3 Modelling

Escoffier (1940) related flow velocity in the inlet to the cross-sectional area of the inlet based on the balance between sediment import by waves and sediment export by tides. He assumed that there is an equilibrium velocity amplitude, U_{eq}. Velocities amplitudes (U) higher than U_{eq} cause net erosion and thus an increasing cross-sectional area of the inlet. Otherwise, for U lower than U_{eq} there is net sedimentation and thus a decreasing cross-sectional area.

The equilibrium velocity is an empirical quantity that depends on the wave activity: an increased wave height increases the value of U_{eq}. Hydrodynamic equations are used to calculate the so called closure curves: curves showing the relation between the inlets cross sectional area (A) and U. This curve is mainly dependent on the incoming tidal wave: higher tidal amplitudes increase the value of U. Herein, Escoffier assumed a uniformly fluctuating basin level. With this model, three different curves can be drawn. The U curve entirely below the line of U_{eq}, indicating no equilibria, one intersection point indicating an unstable equilibrium and two intersection points of which one shows a stable and one an unstable equilibrium. Comparisons between this empirical relation and results of complex process-based morphodynamic models show good agreement (Tran et al., 2012; Tung et al., 2009; Nahon et al., 2012).

When a second inlet is connected to the basin, the first inlet can be affected as part of the tidal prism is captured by the new inlet. When assuming a uniform elevation

of basin water level when calculating the inlet velocity, the extension of the stability concept of Escoffier for multiple inlets leads to the conclusion that no multiple stable equilibria exist and only one of the inlets will remain open (Van De Kreeke, 1990).

However, observations show that stable systems with multiple inlets do exist. Escoffier (1977) for example mentioned the basin near Pine Island (Florida, USA) that has six inlets and appears to be stable. And also the inlets in the Ria Formosa (Portugal) and the Wadden Sea have been in a stable equilibrium for centuries (Van De Kreeke et al., 2008). Five model studies showed methods to derive a stable two inlet system: including a topographic high in the basin between the inlets (Van De Kreeke et al., 2008), including entrance/exit losses near the inlet (Brouwer et al., 2012), accounting for spatial water level variations in the basin (Brouwer et al., 2013) and including non-linearity by adding tidal distortion and residual circulation (Salles et al., 2005) or hypsometry (De Swart and Volp, 2012).

Including spatial variations in basin water level resulted in multiple stable inlets by Roos et al. (2013). Using an idealized model, they explained barrier island length as a function of tidal range and basin area. Results show a strong dependence of the inlets on one another. This exploratory research only included the most important processes to gain general understanding of the stability of tidal inlets. The empirical relation of Escoffier (1940) is combined with a process based hydrodynamic model. When evaluating the existence of stable equilibria, two mechanisms were distinguished: bottom friction is a destabilizing mechanism while pressure differences between the inlets act as a stabilizing mechanism. Because of this, a minimum inlet spacing is found for multiple inlets to be in a stable equilibrium. This minimum inlet spacing, and thus the island length, is smaller for an increasing tidal range and for increasing basin surface area. The inlets were initially imposed by the geometry and the location was, independent of physical processes, randomly chosen. The model only simulates evolution of inlets in terms of closure and was not able to simulate opening of new inlets other than by manually forcing.

1.2 Research set up

1.2.1 Knowledge gap and objective

The widely used concept of Escoffier (1940) and research based on this empirical concept describe the equilibria of tidal inlets. Some complex models can simulate the morphological development of tidal inlets but are not applicable for the long term. On the other hand, idealized models can be used for long-term modelling but because of the strong schematization they only explain general behaviour. The work of Roos et al. (2013) used the concept of Escoffier and demonstrated the existence of multiple stable inlets when accounting for spatially varying water levels. While barrier coast geometry is highly affected by passing storms, the model uses an initially imposed geometry and lacks a mechanism by which new inlets may be formed due to storms. Storm frequency and properties are hard to predict and the link between storms and barrier island breaching is not exactly known. This challenges the modelling of storm-induced barrier island breaching. Because storms occur randomly, including storm-induced breaching in modelling should be done using a probability distribution. According to Wang and Beck (2012), the way to include stochastic events (as storms) in deterministic models is still under discussion as the direct link between storms and barrier island breaching is not known.

There is thus still little knowledge with respect to the long term morphodynamics of tidal inlet systems and its response to external changes. This brings us to the goal of the study.

The goal of this study is to identify the long-term morphodynamic development of storm-induced inlets and their effect on the equilibrium of a tidal inlet system with multiple inlets open in a mesotidal barrier coast.

1.2.2 Research questions

To achieve the research goal, three research questions are formulated. The third question is then split in two:

1. Under what conditions do barrier islands breach, what are the spatial characteristics of the breaches and how do they develop?
2. How can storm-induced breaches be described in a stochastic way and implemented in the idealized model of Roos et al. (2013)?
3. How does the model (as set up in research question 2) respond to the stochastically created breaches and can the inlet stability concept be expressed in a dynamical way?
   (a) What is the effect of storm-induced breaches on the development and equilibrium state of a tidal inlet system?
   (b) What are the most important factors that determine the development of new inlets?

1.2.3 Methodology

The method to answer research question 1 is twofold. First, literature is used to describe the effect of storms on barrier islands and the occurrence and development of these breaches. As second part of the method, data of historical barrier island breaches are used to describe the formation of new inlets. This information is gathered by searching on the internet for both published data of the controlling party of the area where the breach took place, as well as the input and results of studies regarding the subject or area. In the data collection, specific numbers of the time and location of breach is preferred but if unavailable, more general values of the event has been used.

Research question 2 is about setting up the model. The model of Roos et al. (2013) (see section 3.1.1) for multiple tidal inlet systems is an idealized model which is suitable for long term modelling and explaining the general behaviour of the system. This model is used and extended by including storm-induced inlet formation. Because of its history with several island breaches, Long Island (NY, United States of America) is chosen as study area. However, the model can easily be applied to other study areas because of the few input parameters. Because storms occur randomly, storm-induced breaches are implemented stochastically in the model using probability distributions that describe the occurrence, location and size of the breaches. The parameters are defined based on the results of research question 1.

For the last research question, the adjusted model is used to simulate the effect of storm-induced breaches on the tidal inlet system. The evolution of the system over time is analysed to discover patterns. Because of the stochastic nature, a Monte Carlo analysis is performed to find a good representation of the possible outcomes. The analysis is first focussed on the evolution of the entire system for research question 3a, next specific results are studied as evolution of one single inlet for research question 3b. A sensitivity analysis is performed to study the effect of the estimated parameters describing the system.

1.3 Reading guide

Chapter 2 describes the phenomenon of barrier island breaching and gives a historical overview of barrier island breaching. This chapter answers research question 1. Chapter 3 provides a model description and answers research question 2. Chapter 4 shows the model response to the storm-induced breaches and describes the influence of these breaches on the morphodynamics of the tidal inlet system. The conclusions provide answers to research question 3. A discussion is given in Chapter 5 and finally, Chapter 6 contains the conclusions and recommendations.

Chapter 2

Storm-induced inlet formation: theory and historical data

Formation of new inlets is the result of the phenomenon of island breaching that can be caused by strong effects of water and wind, especially during storms. The extreme energy that comes with storms is very influential in coastal systems. Especially vulnerable to storms are barrier islands (Wang and Roberts Briggs, 2015). This chapter provides a background on storms and barrier island breaching including a historical overview of breaches around the world. With that, this chapter answers research question 1.

2.1 Review of island breaching caused by storms

This section describes the formation of a new inlet as a result of a storm. This includes the factors that contribute most to the vulnerability of a barrier coasts and two quantitative classifications developed for predicting and simulating barrier island breaching.

According to Wang and Roberts Briggs (2015), a storm rapidly increases the so-called 'energy of the coast' in form of increased water level, increased wave height and increased wind speeds. These three main aspects of storms affect the tidal inlet system in two ways. First, the existing inlets are affected. Water is pressurized through the inlets which causes a morphological response of the existing inlets and they might increase in size. Second, the storm affects the barrier coast and as a result, new inlets can be formed when islands breach. Breaching can happen both from sea and from basin side. This depends on the wind direction which causes a water level set up or set down in basin and sea (Safak et al., 2016).

The impact of a storm on a barrier island depends on both the hydrodynamic characteristics of the forcing mechanism and the morphological properties of the responding environments (Wang and Roberts Briggs, 2015). In other words, the impact depends on storm properties and topography of the coast. Wang and Roberts Briggs (2015) name the most important factors controlling the forcing mechanisms and responding environments. Topographically, these factors include maximum elevation and width of the island, near-shore morphology, continuity and width of the dune field, beach width and offshore bathymetric characteristics. When looking at the forcing mechanisms, storm intensity, size, track and forward moving speed play a role. A slowly moving storm for example provides more time for the growth of the storm surge and also, the duration of the storm is longer. Both aspects increase the risk of significant morphological changes. According to Wang and Beck (2012), further knowledge is required of the morphological development of coasts by extreme events such as storms. There are two examples of quantitative classifications that

include (some of the) important factors mentioned above: those of Sallenger (2000) and Kraus et al. (2002).

Sallenger (2000) divided the effect of a storm on barrier islands in four regimes with an ascending impact: the swash regime, the collision regime, the overwash regime and the inundation regime. Within this impact scale, storms are represented by water level and coastal topography by dune foot and dune crest elevation. The regimes are clarified in the sketch of Figure 2.1, with R indicating the water level and D the dune height. The water level is defined 'high' when including storm effects and 'low' as the elevation below which the beach is always subaqueous. The dune height is denoted as 'low' at the base of the dune and 'high' at the dune crest.

Swash regime In the swash regime, the beach erodes and sand is transported offshore. After the storm a cross shore sediment transport returns the sand so there is no net change of the beach.

Collision regime In the collision regime, dunes erode and the sand is transported offshore. However, in contrast to the swash regime, the system will not fully recover after a storm and a weaker stable dune is left behind. In some cases the dune will even breach because of the erosion.

Overwash regime In the overwash regime, water overtops the dunes and flows landward. Dunes are eroded and the sand is deposited farther landward. Because this sand will not be fully returned to the dunes that it was originated from, overwash may lead to landward migration of the barrier island.

Inundation regime The last and most extreme regime is the inundation regime. The overwash and inundation cause strong currents on the islands which carry sediments away. When the flood currents as a result of this overwash erode the island enough, the stronger ebb currents can continue carving a channel. These channels can become new inlets. According to Friedrichs et al. (1993), this initial stage of inlet formation is crucial to permanent inlet formation. The newly formed inlets can compete with the old inlets which may result in closure of the old inlets (Friedrichs et al., 1993).

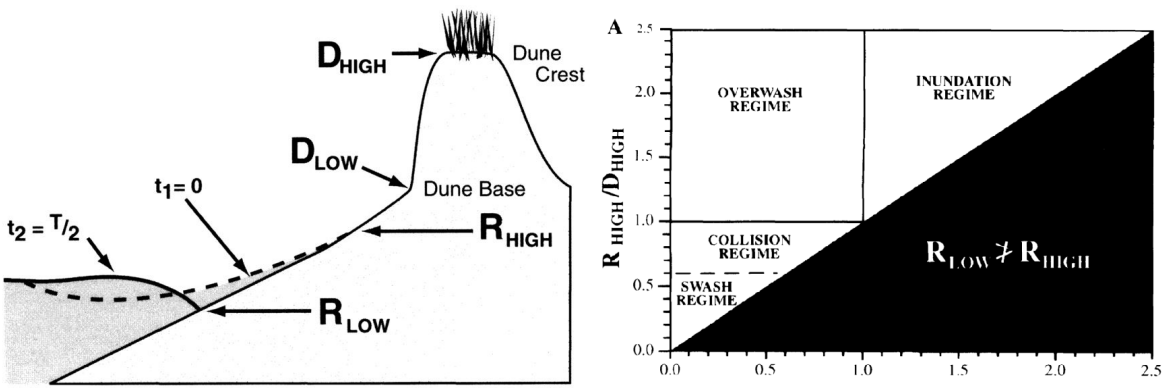

FIGURE 2.1: Sketch showing variables used in impact scale including definition of regimes (Sallenger, 2000)

Alternatively, Kraus et al. (2002) developed a dimensionless 'Breach Susceptibility Index', B, based on surge level and tidal range only. This index in part explains

the tendency of barrier coasts to breach from sea side. The index is defined as:

$$B = S_{10}/R, \tag{2.1}$$

with S_{10} the surge level of a 10 year storm and R the diurnal tidal range while being assumed that the diurnal tide is the highest regular tide. Locations with a value of B larger than one are more prone to breach than location with a value lower than one, this result matches with observed breaching events in the United States. Topography of the coast has not been taken into account in this index.

The quantitative classifications of both Sallenger (2000) and Kraus et al. (2002) explain and predict the breaching concept in general, but are based on little parameters and therefore lack precision. However, accurately simulating short term barrier island breaching has been done successfully by Cañizares and Irish (2008). They set up a model for the area of Long Island, based on both storm characteristics and coastal topography and conclude that the model is capable of realistically simulating overwash and barrier island breaching. This shows that it can be concluded that qualitatively, storm impact to barrier islands is well understood, but further research should be directed towards long term quantitative predictions of storm impact (Wang and Roberts Briggs, 2015).

2.2 Historical overview of breaches

Island breaching is a phenomenon that has occurred frequently in history. Mostly during storms and hurricanes. Well-known areas that experience barrier island breaching are at the eastern coast of the United States of America. This section starts with a summary of the barrier island system at Long Island (New York) that experienced several breaches, including the well-known recent breach at Fire Island during Hurricane Sandy in 2012. The next section gives an overview of historical breaches and their properties.

2.2.1 Example: Long Island

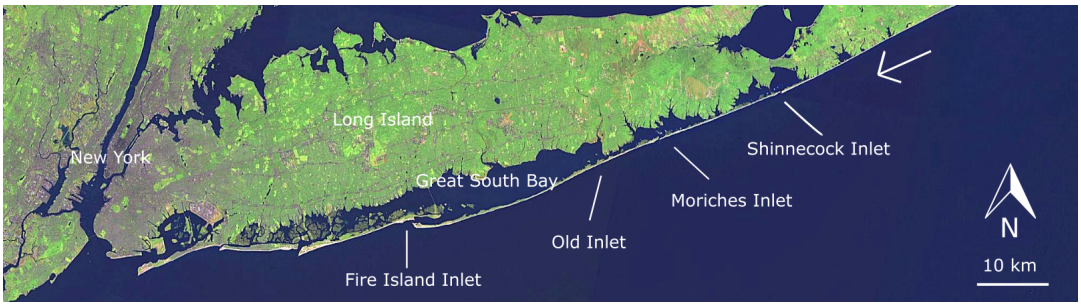

FIGURE 2.2: Map of the barrier system near Long Island, showing inlet locations and with arrow denoting the direction of the littoral drift

A location that shows several examples of barrier island breaching is the barrier coast system south of Long Island – New York, see Figure 2.2. This coastal system is about 120 kilometres long and 10 kilometres wide and consists of 5 major islands

(Google Inc., 2017). The biggest of the basins that is divided from the sea by the islands is the Great South Bay which is 76 kilometres long (Flagg, 2013) and on average 2 metres deep (Schubel et al., 1991). The tides are semi-diurnal (U.S. Army Engineer District New York, 1976) and the system can be classified as mesotidal because of the maximum tidal range of the sea of 2.08 metres (Meteo365, 2017), causing a tidal range in the basin of 0.4 metres (Flagg, 2013). Together with the mean significant wave heights of 1.3 to 1.4 metres, the system is classified as mixed energy - wave dominated (Hayes, 1979). The littoral drift is from east to west at rates of 150.000 m^3 per year (Terchunianf and Merkert, 1995).

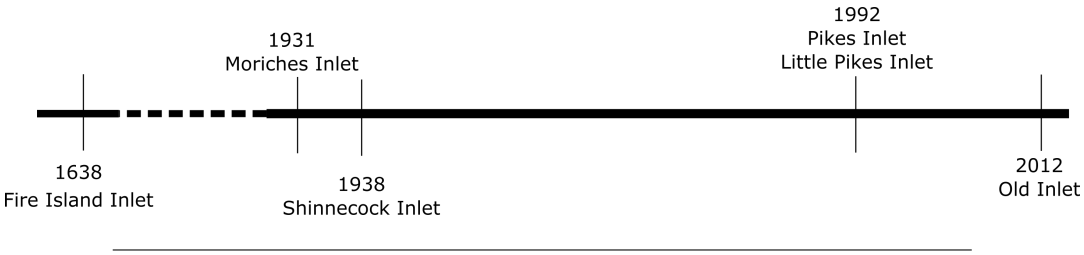

FIGURE 2.3: Timeline showing origin of inlets

The year in which the inlets of Long Island originated is depicted in the timeline in Figure 2.3. In 1638 one of the biggest inlets of the system, which still exists, was created during a storm: Fire Island Inlet. Within the following almost 300 years, six breaches are documented, none of which stayed open. In 1931, a storm caused the formation of Moriches Inlet which did stay open. It was stabilized two decades later: the location and dimensions of the inlet were artificially fixed. In 1938 Shinnecock Inlet and 11 other inlets were created by The Great Hurricane (Mandia, 2017). Shinnecock Inlet is still open due to dredging. According to Kassner & Black (1982), besides the breaches, the hurricane also caused widening of existing inlets as Moriches Inlet (Mandia, 2017).

In 1992, a storm caused two breaches in the most eastern low lying barrier island of Long Island: Pikes Inlet and Little Pikes inlet (Terchunianf and Merkert, 1995). Both breach channels were about 30 metres wide but the overwash area of Little Pikes Inlet was initially smaller. Updrift of both breaches, the coast was stabilized with groynes. Little Pikes Inlet was located directly in the erosional shadow of these groynes. The inlet grew in size up to 1.5 kilometres wide within a year with depths of about 6 metres. About a year after the opening of the breach, emergency measures were taken to close the breach. Pikes Inlet, however, was already closed two months after the storm due to natural and artificial actions. This inlet was located more westward and out of the erosional shadow of the groynes. It therefore received more sediment which accumulated in the breach and led to closure.

The most recent breach in the system is the one at Fire Island in 2012, called: Old Inlet. This specific location experienced breaches several times in the past. Most of the times the inlet quickly closed naturally but until the 1820's it has been an inlet for about 60 years. During hurricane Sandy at the end of October 2012, this Old Inlet was reopened and two other breaches appeared at other locations. The latter two breaches were directly artificially closed whereas because of its location in a federally protected area Old Inlet was left to the natural response of the system (Foderaro, 2016). Photos of the location before and after the breach are shown in Figure 2.4. Old Inlet has been monitored quite extensively during the breach and the

years after, but also during the years before the storm which makes it an interesting and unique study area. Photos of Old Inlet several years after the breaching event can be found in Figure A.1 in Appendix A.

When Hurricane Sandy made landfall in New York, the hurricane was weakened to an extratropical storm with hurricane wind gusts (Blake et al., 2013). The storm still had Beaufort Force 12. The Long Island Barrier islands experienced weaker storm effects with wind speeds of 19 m/s, rated 7 on the Beaufort Scale, and gusts rated 8 on the Beaufort scale. The total sea level rise was 2.6 metres relative to mean sea level (Flagg, 2012). Due to the water level set up and the erosion caused by winds, the water broke through from the sea to the basin. The stream of water that overtopped the dunes eroded a stream for water and carried sediment away. The breach opened at or shortly after the peak in wind speed. From its initial cross sectional area of 100 m^2, Old Inlet grew rapidly in size and reached a stable state after a few months with a cross sectional area of 400 m^2. This cross sectional area is around 10% of the cumulative area of the two main inlets: Moriches and Fire Island Inlet. Correspondingly, the inlet captures 8% of the tidal prism entering the basin (Flagg et al., 2016). While its cross sectional area is stable, the location of the inlet is not, it migrates westward. The inlet depth profiles and its location are shown in Figure 2.4.

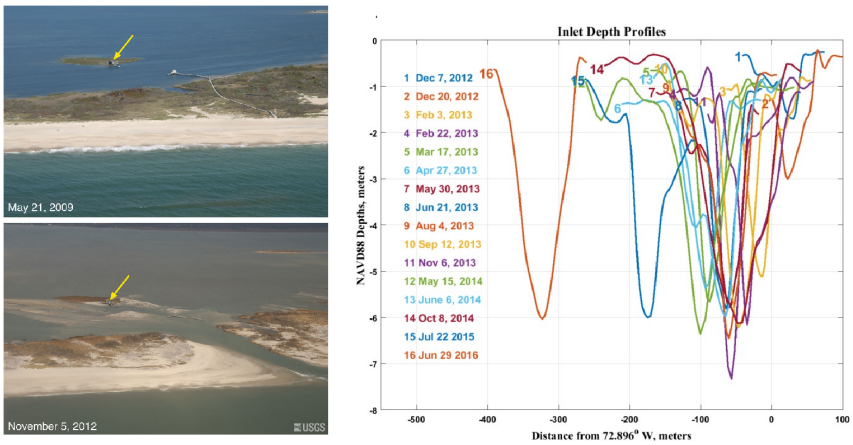

FIGURE 2.4: Left: Old Inlet before and after hurricane Sandy. Right: Development of the cross sectional area of the Old Inlet breach (Flagg et al., 2016), showing westward migration and increasing size of the inlet

The new inlet had some consequences for the area. At the beginning, people were afraid of higher flood risks of the mainland behind the barrier island. Higher water levels were observed in the basin. However, according to Flagg (2013), this was caused by accidental circumstances rather than by the new inlet . Salinity levels in the basin did increase after the new inlet was opened. Another significant result of the new inlet is the improved water quality in the basin. The water entering trough Old Inlet flushes the basin and especially the eastern side of the Great South Bay experiences higher oxygen levels. (Flagg et al., 2016)

2.2.2 Summary and findings of historical breach events

Alike the case of Old Inlet, several barrier island breach events in the past have been documented, some just based on witness observations and others well measured. A

list of some historical breach events together with their properties is shown in Table 2.1.

The breach events included in this table are the events of which storm and breach data could be found. Also, some breach events related to those are included to provide better understanding of the system. The area denoted in this table represents the initial cross sectional area of the breach. This is in some cases the cross sectional area as mentioned in the source. In some cases it is the multiplication of the documented values of the width and depth of the breach. In the cases that only the width of the breach is known, the area is computed by multiplying with the average inlet depth based on the documented breaches of which depth values were available. It should be noted that these cross sectional areas might thus not be accurate and should therefore be interpreted as rough estimates. Nevertheless, they do give insight in the order of magnitude and the range of the area.

A similar uncertainty is present in the value of the Beaufort Force of the storm that caused the breach. These values are best based on specific wind forces at the location and moment of breach. However, these data are in most of the cases not available. In some cases the storm characteristics on the date of breaching provide the most specific values which are therefore used. The Beaufort Force thus represents the force of the storm, on a larger scale than the scale of the breach. General findings based on historical breach events are the following.

Geographical location Most of the breach events took place on islands of the eastern coast of the United States of America. This can be explained because of three reasons. First of all, breaches in the USA are relatively well documented. Probably, breaches in islands elsewhere on the world have occurred but have not been documented and therefore not included in this table. Secondly, there are relatively many barrier islands at this continent: according to Stutz and Pilkey (2011), 7.5% of the world's total number of barrier islands are situated at the Atlantic Ocean of North America. The last reason is that it is an area that experiences heavy storms often, which increases the likelihood of breaching of those islands. According to Hurricane Research Division (2017), on average 1.7 hurricanes make landfall on the USA every year.

Cause of breach Breaches were in all cases induced by at least a storm, so a Beaufort Force of 10. Most of them were created by a hurricane or a weakened hurricane. This Beaufort Scale is based on maximum wind speeds, the local wind speeds near the breach could have been lower. The wind speed associated with the opening of Old Inlet equalled 19 m/s with gusts of 25 m/s, corresponding to a Beaufort Force of 8 and 9 respectively (Flagg, 2012). These forces are lower than the Beaufort the storm was classified to at that moment which was Beaufort Force 12 (Blake et al., 2013).

Number of breaches One single storm event can cause multiple breaches. These breach-channels can be close to each other, as the three channels on Hatteras Island, North Carolina which were created by Hurricane Isabel in 2003 (U.S. Geological Survey, 2009). However, they can also be further away. During Hurricane Irene in 2011, at the same string of barrier islands, two breaches developed on two different islands (Clinch et al., 2012). At maximum, twelve new inlets caused by one storm are documented. These developed during The Great Hurricane of 1938 and all but Shinnecock Inlet closed quickly after the storm.

Location of breach Literature suggests that the location where a breach occurs is one of the weakest spots of the system, often because that part is low lying or narrow (Wang and Roberts Briggs, 2015). There are many examples of historical inlets that have been closed but reopened during a storm. Though these inlets were closed, the area was still low lying and narrow and thus vulnerable to storms. Old Inlet for example has also been open for 60 years in the eighteenth century (Flagg, 2013). Also Pea Island Inlet opened in 2001 almost exactly at the location were an inlet has been in 1932 (Clinch et al., 2012).

Breach size The cross-sectional area of the breaches ranges between 50 and 500 m^2 with different aspect ratios.

Widening of existing inlets Besides the opening of new inlets, storms often caused widening of existing inlets. The storm caused a water level set up on the sea side that initiated a larger tidal prism than the tidal inlet normally has to accommodate. For example: Pea Island Inlet quadrupled in size during Hurricane Sandy (Safak et al., 2016). Also, Moriches Inlet was widened when Hurricane Sandy arrived and created Old Inlet.

Natural and human-induced evolution of system Many of the newly formed inlets closed naturally and within a few months after the storms. Several inlets did not close naturally and stayed open for the long term or were closed artificially out of emergency. Considerations of closing or even dredging to keep open depend often on human interest. For example fear of rising basin water level and flooding of the mainland can be a reason to close the inlet. This was the case at Long Island (Flagg, 2013). A road on Pea Island was cut by the pea island breach which made one part of the island inaccessible (Clinch et al., 2012). A bridge was built to cover the breach, but closure of the breach solved the problem. Human interests, such as navigation, could also lead to measures to keep the inlets open by dredging or stabilizing. This happened with some of the inlets of the system of the Long Island Barrier Islands (Vogel and Kana, 1984)

The breach events of which the initial breach cross sectional areas as well as storm intensity data are known, are plotted in Figure 2.5. This figure shows the relation between storm intensity (expressed as Beaufort force of the storm) and initial breach area. The plot shows that breaches only occur during storms with Beaufort forces higher than 10. It also shows the range of breach sizes. The cross sectional area ranges between 38 and 510 m^2 with a mean value of 140 m^2. No significant relation between storm intensity and breach size can be found.

2.3 Subconclusion

The occurrence of a breach depends on both hydrodynamic characteristics (as wind speed and direction) and morphological properties (as height and width of the island). Two quantitative classifications have been developed to predict breaches (Kraus et al., 2002; Sallenger, 2000) , both including just some of the characteristics. Breaching occurred frequently in history but often not (well) documented. Therefore, the breach data could not be linked to the two indexes. It is found that breaching only occurs during storms of at least Beaufort Force 10 and that the cross sectional area of these breaches vary between 50 and 510 m^2.Based on available data no relation is found between the Beaufort Force of the storm and the cross sectional

TABLE 2.1: Historical barrier island breach events

Location			Date	Cause	Beaufort Force	Area (m2)	Status	Source
US - New York	Long Island Barrier Islands	Fire Island - Old Inlet	29-10-2012	Hurricane Sandy	12	100	Open	Flagg et al. (2016)
		Fire Island - Smith Point					Closed Artificially	
		Westhampton breach					Closed Artificially	
		Moriches Inlet	4-3-1931	Nor'Easter / extratropical storm	11	500	Open Stabilized	Vogel and Kana (1984)
		Shinnecock Inlet	1938	The Great Hurricane			Open Stabilized	Cañizares and Irish (2008)
		Pikes Inlet	dec-92	Nor'Easter	10	51	Closed Naturally	
		Little Pikes Inlet				51	Closed Artificially	
US - New Jersey	Mantoloking		2012	Hurricane Sandy	12	85	Closed Artificially	FEMA (2013)
US - Maryland	Assateague Island	Ocean City Inlet	23-8-1933	Chesapeake-Potomac Hurricane	11	228	Open Stabilized	MacIvor (1998)
		North Inlet	1962	Nor'Easter	11	146,4	Closed Artificially	
		South Inlet					Closed Naturally	
US - North Carolina	Outer Banks barrier islands	Oregon Inlet	1846	Hurricane			Open	Mallinson et al. (2008)
		Hatteras Inlet					Open	
		Drum Inlet	1933	Major Hurricane			Open	
		Buxton Inlet	1962	Ash Wednesday storm			Closed Artificially	
		Hatteras Island - Isabel Inlet West	18-9-2003	Hurricane Isabel	12	63,6	Closed Artificially	Wamsley et al. (2010)
		Hatteras Island - Isabel Inlet Middle				70	Closed Artificially	
		Hatteras Island - Isabel Inlet East				300	Closed Artificially	
		Pea Island - New Inlet	6-3-1932	Nor'Easter	10	39,1	Closed Naturally	Clinch et al. (2012)
						510	Closed Unknown	
						38,25	Closed Naturally	
						38,25	Closed Naturally	
						38,25	Closed Naturally	
		Rodanthe - Mirlo Beach	27-8-2011	Hurricane Irene	11	112,5	Closed Naturally	Safak et al. (2016)
						0	Closed Naturally	
US - Alabama		Pine Beach	09-04	Hurricane Ivan	12	85	Closed Unknown	U.S. Geological Survey, 2016
Portugal	Ria Formosa Barrier Islands	Cacela Peninsula	1996		10	45,5	Closed Artificially	Matias et al. (1999)
			2010		10	102	Open	Google Inc. (2017)

area of the breach. Sometimes multiple breaches are created during a single storm. There are only few examples of breaches that developed naturally into an open inlet. Most breaches closed (either naturally or artificially) or were artificially fixed by construction of jetties.

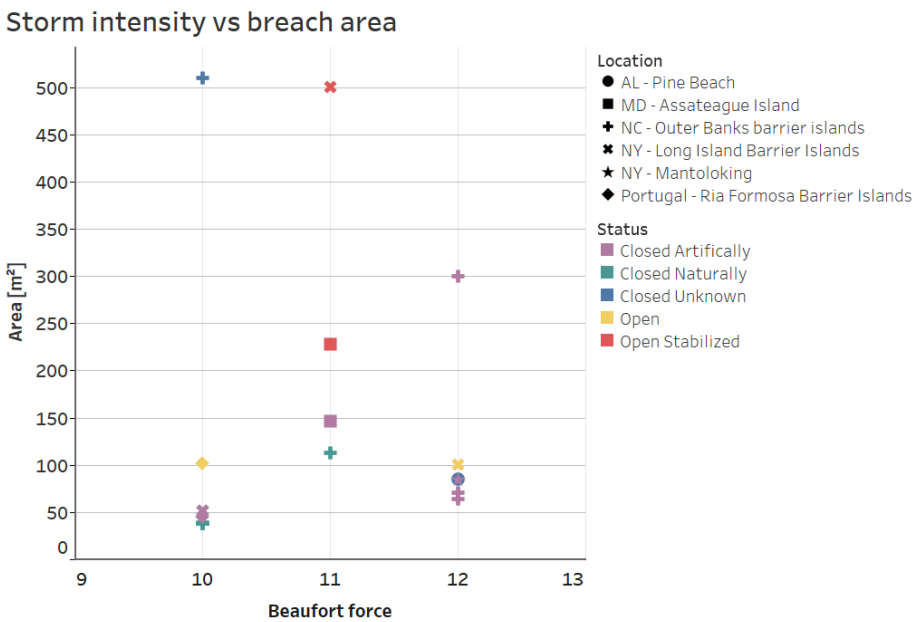

FIGURE 2.5: Plot of storm force (Beaufort) vs initial cross sectional are of historical breaches.

Chapter 3

Model set-up

This chapter describes the model set up with a focus on including storm-induced breaches. This chapter answers research question 2.

3.1 General model set up

The exploratory model of Roos et al. (2013) is the basis for this research. This idealized model is chosen because the simplification allows to investigate general behaviour of the system and to model long term evolution while not taking too much computation time. The study of Roos et al. (2013) showed that this model is able to simulate a stable equilibrium with multiple inlets open and is therefore suitable to use in this research.

3.1.1 Model formulation

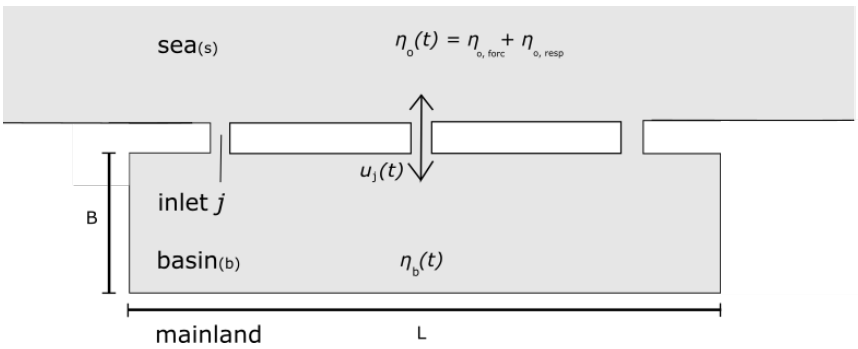

FIGURE 3.1: Model geometry of tidal inlet system with arrow denoting flow between basin and sea through an inlet as forced by an incoming tidal wave

An example of the two dimensional geometry of the system is as sketched in Figure 3.1. It consists of J inlets with depth h_j and width b_j connecting a single rectangular basin with uniform depth (h_b) to the sea. Note that for visibility the figure is not on scale. We start with 1 inlet, initially specified at a random location and with cross-sectional area, A_j. A fixed shapefactor ($\gamma^2 = h_j/b_j$) for all inlets is used initially and throughout their evolution.

The model describes the evolution of the system based on the morphological loop as already shown in Figure 1.2 in section 1.1. The hydrodynamics of the waves and tides determine the amount of sediment that is being transported in and out of

the inlet, which changes the cross sectional area of the inlet. The hydrodynamics adjust to the new morphology. Escoffier coupled sediment transport to morphological changes so the morphological changes can directly be calculated with known hydrodynamics. The model can thus be split in two parts, the hydrodynamics and the morphodynamics.

Hydrodynamics are modelled as follows. The system is forced by an incoming tidal wave that causes a water level variation in the sea in time (η_s). Because of the pressure difference between basin and sea, water flows with a certain speed (u) through the inlets with length l and changes the water level in the basin (η_b). The flow velocities in the basin, sea and inlets are calculated analytically using a process based hydrodynamic model. The time scale of hydrodynamics is in the order of a day. In the sea, bottom friction is neglected while in the basin and the inlets it is not. The uniform flow velocity in the inlets satisfies the momentum equation:

$$\frac{\partial u_j}{\partial t} + \frac{r_j u_j}{h_j} = -g\frac{\langle \eta_s \rangle_j - \langle \eta_b \rangle_j}{l} \tag{3.1}$$

Here, r_j is the linear bottom friction coefficient in inlet j, h_j the water depth in inlet j, g the gravitational acceleration and η the surface water elevation at the basin side (denoted with subscript b) and the sea side (denoted with subscript s) of inlet j. The angular brackets $<>_j$ indicate averaging over the inlet mouth. The cross-sectionally averaged flow velocity in the inlet (u) is assumed to be a single scalar quantity for each inlet. The surface elevation depends on the velocity in the basin/sea and the sea and basin impedances that express the influence of flow through inlet q on the surface elevation at inlet j.

$$\frac{\partial \boldsymbol{u}_s}{\partial t} = -g\nabla\eta_s, \qquad \frac{\partial \eta_s}{\partial t} + h_s(\nabla \cdot \boldsymbol{u}_s) = 0 \tag{3.2}$$

$$\frac{\partial \boldsymbol{u}_b}{\partial t} + \frac{r_b \boldsymbol{u}_b}{h_b} = -g\nabla\eta_b, \qquad \frac{\partial \eta_b}{\partial t} + h_b(\nabla \cdot \boldsymbol{u}_b) = 0 \tag{3.3}$$

In these equations, $\boldsymbol{u}$ is the depth-averaged flow velocity vector with components u and v in x- and y-direction respectively. r_b is the linear bottom friction coefficient it the basin. The bottom friction in both basin and inlets depend on the solution:

$$r_b = \frac{8c_d U_b}{3\pi}, \qquad r_j = \frac{8c_d U_j}{3\pi}, \tag{3.4}$$

with drag coefficient c_d and velocity amplitude of the basin U_b and inlet U_j. U_j directly follows from the hydrodynamic solution. U_b is derived by integration over the entire basin and dividing by the basin area. Because of the dependency of the bottom friction on the velocity amplitude, an iterative approach has to be used when solving the hydrodynamic equations. Using under relaxation this iterative approach continues till the solution matches the initial guess of the velocity scale used to calculate the bottom friction in inlets and basin.

After solving the hydrodynamic equations, the inlet morphodynamics can be computed. The morphodynamics are described by Escoffiers inlet evolution which is based on the imbalance between sediment import and export. The cross-sectional area A_j of inlet j evolves according to:

$$\frac{dA_j}{dt} = \frac{\kappa U_{eq}^n}{l}\left(\left(\frac{U_j}{U_{eq}}\right)^n - 1\right) \tag{3.5}$$

In this equation: κ is constant indicating the sediment im- and export, U_{eq} the equilibrium velocity amplitude, l the length of the inlet channel and U_j flow velocity amplitude in inlet j. The timescale of the morphodynamics are in the order of years. The morphodynamic evolution is solved numerically, with time step Δt, using Forward Euler discretisation. The model allows for merging of inlets by keeping the total area constant and changing the inlets depth and width according to the shapefactor.

3.1.2 Parameter settings

The parameters used in the model are as listed in Table 3.1. The values are based on the location of Long Island, see section 2.2.1.

TABLE 3.1: Model parameters of Long Island barrier island system

Parameter	Symbol	Value LongIsland	Physical unit
Tidal amplitude	Z	0.75	m
Tidal Frequency	ω	1.4×10^{-4}	rad/s
Basin Width	B	4×10^{3}	m
Basin Length	L	76×10^{3}	m
Basin Depth	h_b	1.3	m
Sea Depth	h_s	10	m
Inlet Length	l	1.2×10^{3}	m
Initial Inlet Depth	h	7.7	m
Initial Inlet Width	b	0.26×10^{3}	m
Inlet Shape factor	γ^2	0.03	-
Initial number of inlets	J	1	-
Equilibrium velocity	U_{eq}	1	m/s
Sediment import	M	0.15×10^{6}	m^3/year
Timestep	Δt	0.5	year
Simulation time	T	600	year
Drag coefficient	c_d	2.5×10^{-3}	-
Mean breach width	b_b	0.1×10^{3}	m
Standard deviation breach width	σ_b	70	m
Breach frequency	f_b	1/20	per year

3.2 Storm-induced breaches - Stochastic modelling

Because storms occur randomly, we treat storms as a stochastic process in modelling. A way do deal with stochastic processes in a model is using a Monte Carlo simulation. The process of a Monte Carlo simulation proceeds following five steps (Fenton and Griffiths, 2008). First of all, a distribution of the random parameter has to be estimated based on observations from the real world. When this distribution is decided, the random field can be defined. A random number generator uses this random field and one realization of the system can be performed. The next step is to evaluate the response of the system to the random input. This way, a deterministic model is run with stochastic input. The last two steps are repeated as many times as necessary and the number of occurrences of a particular response are recorded. From this, a histogram can be formed which forms the estimate of the probability distribution of the system response. The outcomes of the simulations can now be treated

statistically which gives an indication of the chances an outcome would occur. These chances form a probability distribution and for example the mean, minimum, maximum and variance of the output can be determined. While increasing the number of realizations will increase the accuracy, a major disadvantage of the Monte Carlo simulation is that the computational time will increase as well (Lerche and Mudford, 2005). A balance between these two factors has to be found. In this study it is chosen to do 10,000 Monte Carlo simulations.

Three probability distributions are used to describe the breach characteristics. Every time step it is randomly chosen from the first distribution whether a breach will appear. If there is a breach, the location of each breach will be chosen based on the second distribution. The last distribution then decides on the size of the breach.

Appearance of breach The first distribution has only two outcomes: a storm occurs that is causing breach(es) or no storm occurs that is causing a breach. This distribution is based on historical events that record around 1 storm every 20 years. Historical observations show in most cases a single breach but multiple breaches are recorded as well. Therefore, the number of breaches that occurs when a storms passes is randomly chosen with 66% chance of 1 breach and descending chance of 2, 3, 4 or 5 breaches.

Location of breach The distribution that determines the location of the breach is uniformly distributed over all islands. The breach is not allowed to overlap with an existing inlet at the moment it is created. According to historical observations and the theory of Sallenger (2000), it is more likely for a breach to occur at a location where the island and dune row is smaller and lower. This location however differs per system. It depends on erosion history and thus on hydrodynamics near the islands. No general location is found that is more susceptible to breaching. Because of the purpose of the model: explaining general behaviour of the model, it is not useful to further specify the distribution of the breach location.

Breach size The third distribution determines the breach width. The cross sectional area can then be computed because of the fixed depth/width ratio. Based on historical data the mean and standard deviation of the breach width is chosen and a normal distribution is created with these values as normal distributions tend to describe natural phenomena quite well. Negative values and breaches smaller than 25 metres wide are unrealistic and therefore filtered out of the distribution by repeating the width generation process. The black line of Figure 3.2 shows the normal distribution with mean of 100m and standard deviation of 70 metres. Because breach sizes smaller than 25 metres are filtered out the distribution changes and is like the histogram shown in grey. As a result, the mean value (118 metres) is higher and the standard deviation (56 metres) lower.

3.3 Subconclusion

The model of Roos et al. (2013) is extended by including storm-induced breaching. This way, the model is able to simulate the entire evolution of inlets and the tidal inlet system, from opening to closing. The initial geometry consists of a single inlet and every time step there is a chance that a storm passes that creates a breach.

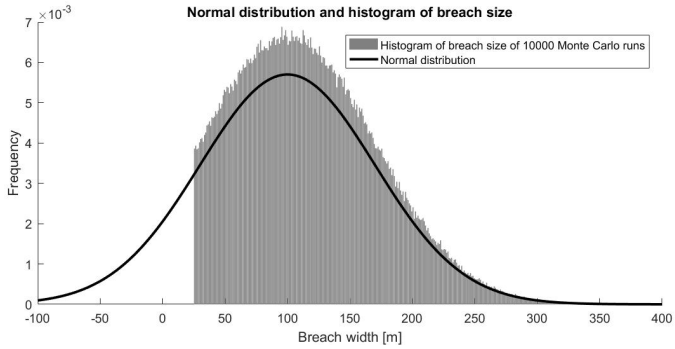

FIGURE 3.2: Example of probability distribution: normal distribution with mean of 100 and standard deviation of 70. Grey histogram displays the histogram of breach size of all breaches of 10,000 Monte Carlo simulations

Three probability distributions are implemented that determine the properties of the breach. The first distribution is used every time step to choose the amount of breaches. The second one is uniformly distributed and is used to specify the location of the breach. Finally, the breach size is based on an adapted normal distribution. Because of the stochastic input used in the deterministic model, a Monte Carlo simulation is used to analyse the model results.

Chapter 4

Results

This chapter gives the results of the modelling and answers research question 3, 3a and 3b. The chapter starts with the results of an example run. Next a Monte Carlo analysis of 10,000 runs has been performed to give a statistical description of the model results. These results are then compared to the situation without storms. Next, a more in depth analysis of the initial evolution of a new inlet is given: what factors contribute most to whether a breach becomes an inlet or closes naturally? The last section includes a sensitivity analysis to find the most important parameters.

4.1 Model response - example run

This section shows the results of a single run. Note that because the stochastic elements, this is just one of the many possible outcomes of the model.

4.1.1 Evolution of entire system

Figure 4.1A shows the result of a single run of the tidal inlet system model. During these 600 years, several storms have occurred that created 33 breaches, made visible as coloured dots. Some of these breaches decreased in size immediately after they opened and close within several years. Others grow in size and become inlets. The width of the black lines indicate the width of the inlets, showing differences in width between the inlets but also increase and decrease of the inlet width in time when being influenced by other inlets of the system.

4.1.2 Inlet area per inlet

A closer look at the development of each inlet of the example run is shown in Figure 4.1B, showing the evolution of the cross sectional area of each inlet in time. The colour of the lines gives the location of the inlet with similar colours indicating inlets close to each other. For breaches that become inlets, the Figure indicates a dependency between the cross sectional area of inlets. When a breach develops into a new inlet, the total cross-sectional area of pre-existing inlets decreases. However, the time scale for inlets to decrease in size is longer than for breaches to grow the same amount in area. That is, the new inlet may have reached an equilibrium state while adjacent inlets are still decreasing in size towards their new equilibrium value as a result of the new inlet. This phenomenon is made clearly visible in Figure A.4 in Appendix A. A good example of reaction of the system to breaches can be seen at t = 128.5y, highlighted with a box in Figure 4.1. Four breaches have been created at locations 16604, 26506, 27368 and 47771 m. The first two close immediately and the other two become new inlets. The tidal prism of the pre-existing inlets decreases as

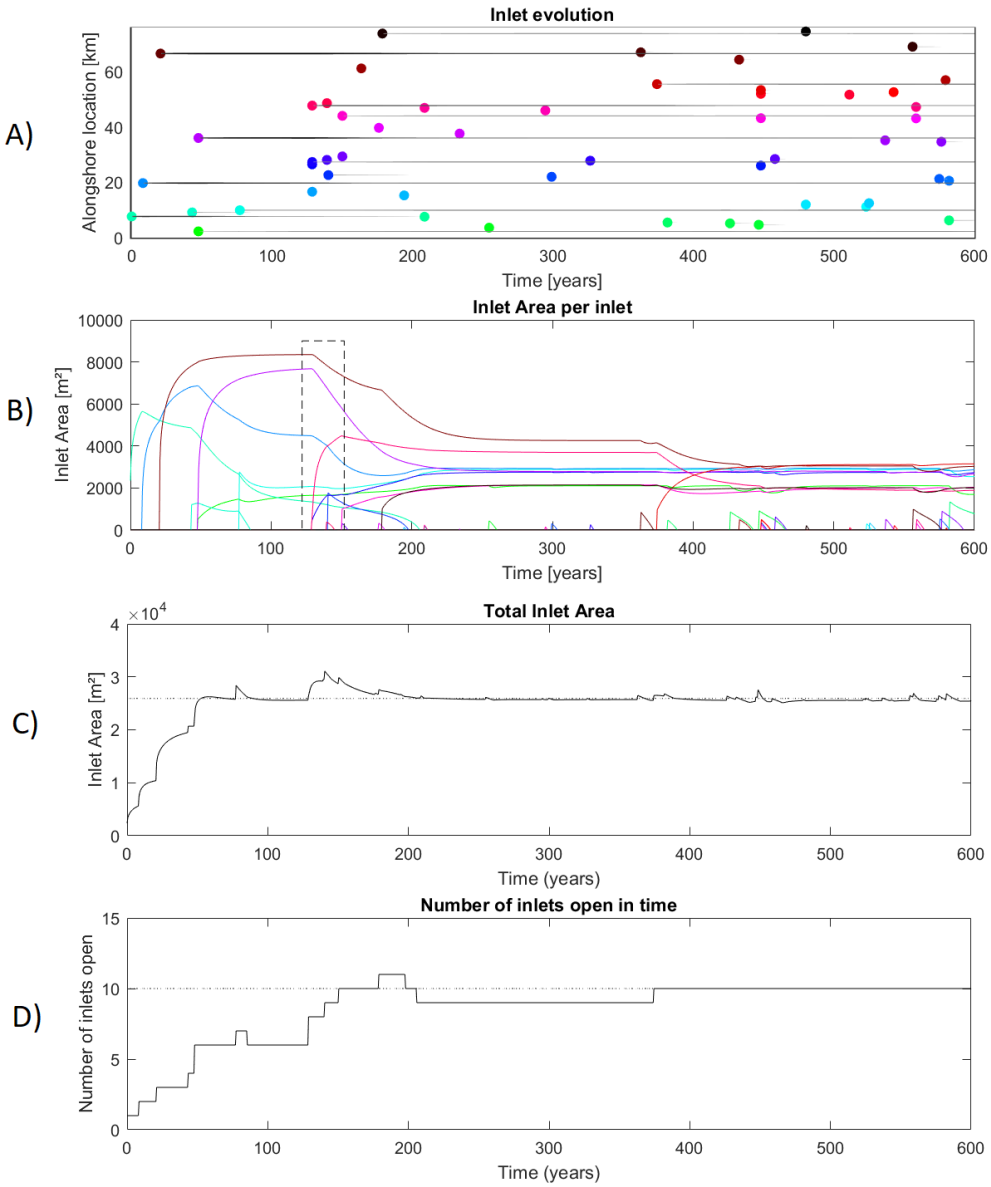

FIGURE 4.1: A) Evolution of tidal inlet system in time. With thickness of the line showing inlet width and dots indicating a breach. B) Cross-sectional area per inlet in time. The colours of the lines match with figure A and indicate location of inlet. C) Total inlet area in time. D) Number of open inlets in time

a result of the new inlet and the figure shows that the three adjacent inlets therefore decrease in size.

4.1.3 Equilibria

A total inlet area is defined as the sum of the area of all inlets:

$$A_{tot} = \sum_j A_j, \tag{4.1}$$

which varies throughout each simulation. A_{tot} gives a measure to analyse the evolution of the whole tidal inlet system. Figure 4.1C shows this total cross sectional area on the vertical axis. The time is indicated by the horizontal axis. The dotted line indicates the average value of the total inlet area over the last 450 years. These results show that the total inlet area evolves towards an equilibrium value which is close to the value of the mean. The first years when the total area is low, the area increases in time until it reaches the equilibrium value. The next years, the value of A_{tot} fluctuates around this equilibrium value. The equilibrium is stable, after a perturbation in the system, it returns to its equilibrium value of the total area. In other words, when a storm causes an increase in the total area by widening existing inlets and creating breaches, at least one of the inlets will decrease in size after this event so the total area will move back to its equilibrium value again.

A similar graph is made for the number of open inlets through time (N_{tot}), shown in Figure 4.1D. Inlets that exist less than 30 years have not been counted, this way breaches that close and hardly affect the system are filtered out. The number of open inlets fluctuates through time. The first hundreds of years, the number of open inlets increases. But this increase is flattened through time with the system reaching a seeming equilibrium number of open inlets after 400 years.

4.2 Monte Carlo Analysis

Because most of the breaching input parameters are randomly chosen, multiple simulations should be performed to analyse the behaviour of the system. The more simulations, the more possible outcomes can be analysed and the more accurate the conclusions can be drawn.

4.2.1 Equilibria

Performing an ensemble run consisting of 10,000 simulations gives 10,000 graphs as in Figure 4.1. A plot of these can be found in Figure A.2 and Figure A.3 in Appendix A. For all of these runs, the mean value for both inlet area as number of open inlets is determined over the last 450 and 200 years respectively. Section 4.2.2 elaborates more on the choice of these two intervals. A Monte Carlo analysis produces a histogram of these mean values as a result, these are plotted in Figure 4.2 with statistical details in Table 4.1. The total inlet area is on average 25.8 $\times 10^3$ m^2. Deviations from this mean are small with the longest tail of the distribution being on on the site with lower values. The variance in the total number of open inlets is bigger with the number of open inlets ranging from 8 to 14. Using the data of Table 4.1, normal distributions are fitted to the results and plotted in the same figure. For N_{tot} this appears to be a good fit. Because the histogram of A_{tot} shows a tail on the left, the distribution seem to be less of a good fit to this quantity. Therefore, also a normal distribution

with standard deviation of 147 m^2 is plotted. Apart form the extreme low values, this distribution seems to be a good fit to the results.

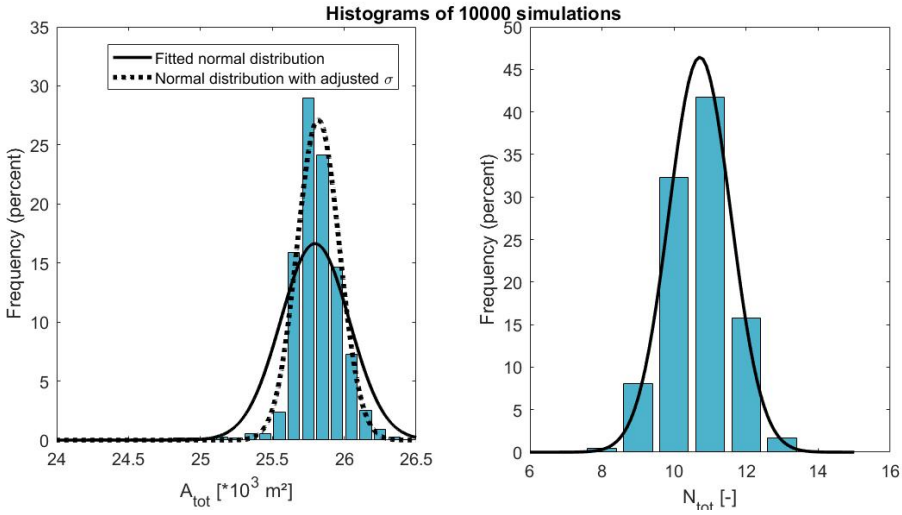

FIGURE 4.2: Histograms of 10,000 simulations showing equilibrium value of total inlet area and number of open inlets

TABLE 4.1: Statistics of Monte Carlo ensemble, total inlet area and number of open inlets

	Mean	Std	Min	Max
A_{tot} [m^2]	25.8 $\times 10^3$	232	21.7 $\times 10^3$	26.4 $\times 10^3$
N_{tot} [-]	11	0.85	7	14

4.2.2 Evolution in time

In Figure 4.3, the average evolution of the system in time of 10,000 simulations is plotted. The blue line shows the average total area of the inlets and the red line the number of open inlets. Both quantities show an increase in time until it reaches a certain value and then stop increasing. For the total inlet area this value is called the equilibrium value of the total inlet area of the system, for the number of open inlets this is the maximum number of open inlets. Based on the moment the equilibrium and maximum values are reached, three stages can be identified.

Stage I: A_{tot} and N_{tot} adjustment - 0-150y The system has reached none of its equilibrium values.

Stage II: N_{tot} adjustment - 150-400y The system has reached its equilibrium value in total inlet area (A_{tot}) but has fewer inlets than the maximum number of inlets (N_{tot}) .

Stage III: Saturated coast - 400-600y The system consists of the maximum number of inlets. Both (A_{tot}) as (N_{tot}) have reached its equilibrium value.

In Figure 4.3, a slight overshoot in inlet area is visible around t=150y. For several years, A_{tot} is slightly higher than the equilibrium value. This is the result of the phenomenon as discussed in section 4.1.2. The time-scale of increasing in size is

shorter than the one of decreasing in size. Therefore the total inlet area is higher the first years after a breach is created that grows to an inlet. In Stage I, more breaches stay open than in the other stages (see also section 4.4.1) which results in a slight overshoot in total inlet area which will be restored several years later.

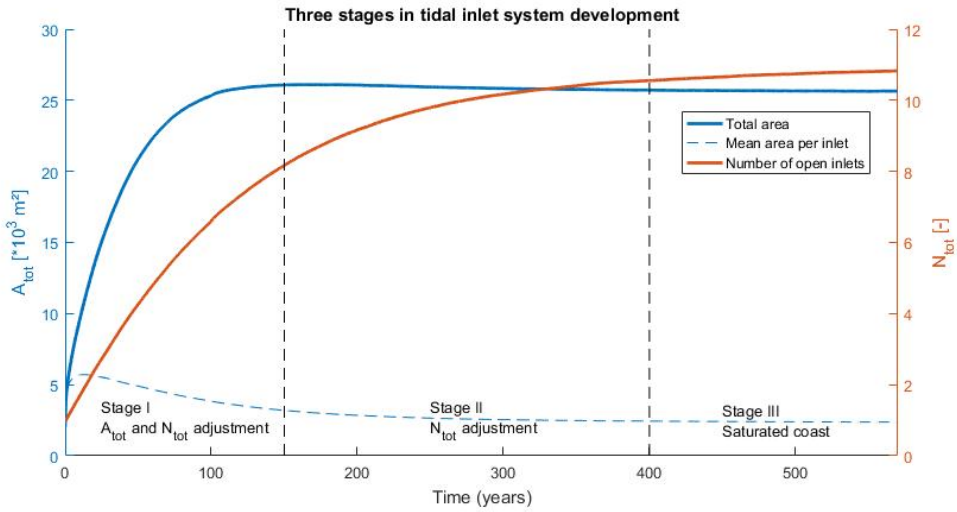

FIGURE 4.3: Evolution of number of open inlets and total inlet area in time, showing three stages

4.2.3 Analysis of closing inlets

Because of the maximum number of open inlets of the system, most inlets that have been created will close (eventually). A distinction between all inlets that closed can be made. The first group, marked as 'initial size decrease', are the inlets that decreased in size in the first morphodynamic time step after opening. N_d is the number of inlets in this group. Apparently these inlets did not have potential to become a stable open inlet in the state of the system of that moment. The other group are the inlets that increased in size in the first time step after opening, marked as 'initial size increase'. N_i is the number of inlets in this group. These inlets grew in size and generally stayed open for years. Only because they got affected by the opening of new inlets, they eventually closed. An decrease ratio (R_d) and increase ratio (R_i) are defined :

$$R_d = \frac{N_d}{N_i + N_d}, \qquad R_i = \frac{N_i}{N_i + N_d} \tag{4.2}$$

Note: this definition is based on the evolution in the first time step after creating only. It gives a good indication of the tendency of the new inlet, however, there are examples of inlets that evolve to an equilibrium state even though they were marked as 'initial size decrease'. This is especially the case for inlets that have a large initial width that might be larger than the equilibrium width. Based on observations during modelling it can be stated that in most cases the definition can be used as most inlets of N_d continued the closing process and most of N_i grew in size and stayed open at least until a perturbation changed the system.

Figure 4.4 shows an histogram of the lifetime of inlets. The lifetime is up to 600 years but the frequency is that low that it is barely visible in the histogram, the Figure therefore only shows lifetimes up to 100 years. Inlets that were open at the end of the

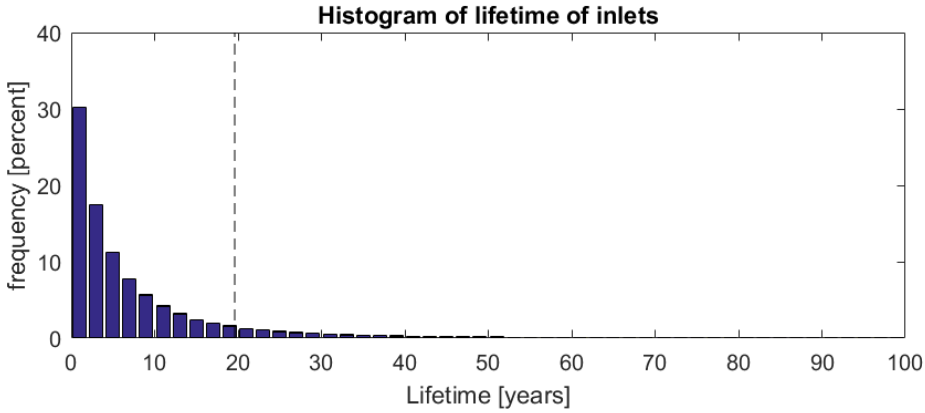

FIGURE 4.4: Histogram of lifetime of inlets for ensemble run with dotted line indicating the average

simulation are not included. For this ensemble run, the average lifetime of inlets of this rather skewed distribution is 19.6 years. Most inlets have a shorter lifetime but the tail of the histogram continues until 600 years. Though the frequency of inlets with a longer lifetime is low, the mean value is clearly affected.

While including all inlets of the ensemble run, R_d is 0.76. So 76% of all inlets decreased in size right after the breach occurred. When splitting the results in the two groups (the 24% that increased and the 76% that decreased), a clear difference in lifetime is visible. For the group that decreased in size the first time step, the mean lifetime is 9 years. For the other group it is much higher: 201 years. The lifetime also differs among the three stages with a mean lifetime of 68 years in stage I, 13 years in stage II and 8 years in stage III. This is best visible in a cumulative distribution function as shown in Figure A.6 in A.

4.3 Comparison to model without storm-induced breaches (Roos et al., 2013)

In this section, we compare the results of the case with storm-induced breaches, as given in the previous sections, with those of the model without the ability to create new inlets, as performed by Roos et al. (2013). This consists first of all of a comparison of the equilibrium value of A_{tot} and $Ntot$. Next, the sensitivity of these numbers to basin width and tidal range is determined and compared to the results of Roos et al. (2013)

4.3.1 Equilibrium values

The model without breaching uses the same input parameters as specified for the model with breaching, except the input for the initial number of inlets. The initial number of inlets is chosen to be 75, this way an inlet is present every kilometre. When running the model, the competition between these inlets cause inlets to close and an equilibrium will be found.

The evolution of the total inlet area and number of open inlets in time is shown in Figure 4.5. In both cases, it is shown that the system reaches an equilibrium after sufficient time: an equilibrium for the total inlet area and the maximum amount of open inlets. The result for the case without breaching and the mean value resulting

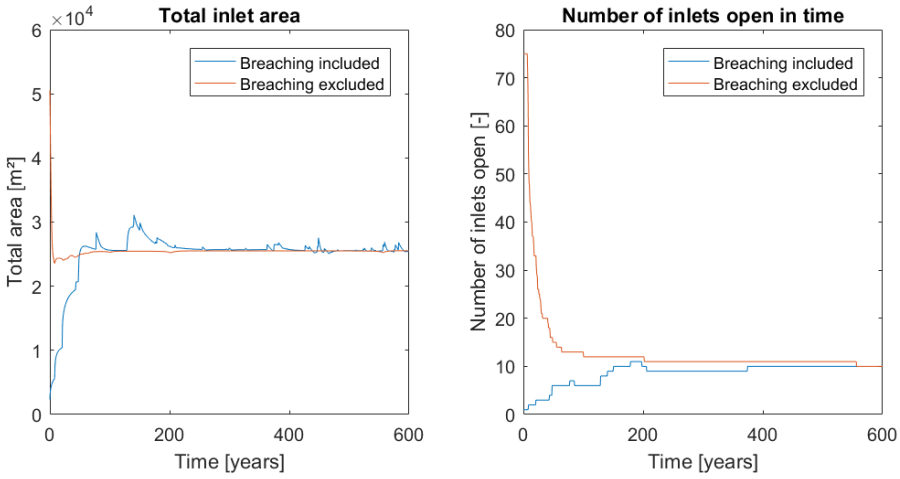

FIGURE 4.5: Evolution of total inlet area and number of open inlets for example runs with and without storm-induced breaching

from the Monte Carlo simulation for the case with breaching (see also section 4.2.1) are shown in Table 4.2. The results for the model with and without storm-induced breaches are very similar: the equilibrium state of the system is almost identical. This means that the model is insensitive to the initial state and that including storm-induced breaches does not affect the equilibrium state that the system tends to reach. The slightly higher total area for the case with breaching can be explained by the fact that due to breaching the total area slightly increases every now and then. The system will restore the equilibrium state so the area of the inlets will decrease, however this takes time so the mean total area increases due to breaching. The number of open inlets is higher for the situation without breaching. This is the result of the initial geometry with 75 inlets ($N_{IC} = 75$). This way, the ideal situation can be simulated with inlets at those locations such that the distance between inlets is exactly the minimum inlet spacing. When starting with one inlet and allowing for breaching, the chance is simply much smaller that this optimal configuration will occur. Distances between inlets may therefore be bigger than the minimum inlet spacing and the total number of inlets is thus smaller. Because of this difference, A Monte Carlo simulation is performed for the situation with breaching but with the initial condition with 75 inlets. These results correspond even better to the one without breaching.

TABLE 4.2: Comparison model results with and without allowing for breaching

	$N_{IC}[-]$	A_{tot} [m^2]	N_{tot} [-]
Breaching excluded	75	25.5×10^3	11.1
Breaching included	1	$\mu = 25.8 \times 10^3, \sigma = 232$	$\mu = 10.7, \sigma = 0.85$
Breaching included	75	$\mu = 25.6 \times 10^3, \sigma = 36$	$\mu = 11.1, \sigma = 0.84$

It can be noticed that the maximum number of open inlets is not an integer. This is a consequence of the averaging over multiple runs. The maximum number of inlets is thus 12, though depending on the location of the inlets and the assumption that inlets can not migrate, it often happens that 11 or 10 is the maximum.

4.3.2 Sensitivity to basin width and tidal amplitude

The study of Roos et al. (2013) concludes that the number of inlets depend on the tidal range and the basin width. To determine whether this also holds for the model that includes breaching, a sensitivity analysis of basin width and tidal amplitude is performed. Five different values for both parameters have been chosen: one as used in the regular simulation and two higher and two lower values. For both parameters, the effect on the total inlet area and the number of open inlets is searched for by taking the mean of 100 Monte Carlo simulations. The total inlet area and number of open inlets are determined the same way as in the regular simulation, by using the the equilibrium value. The output values are normalized by dividing by the value of the regular run.

The results are shown in Figure 4.6. An increasing tidal range leads to an increase in total inlet area and an increase in the number of open inlets. Both increases seem to be linear. The results for the basin width show a similar result. For both tidal amplitude or basin width, A_{tot} is more sensitive to changes than N_{tot}. These results coincide with the model results without storm-induced breaching as well as the theory of Stutz and Pilkey (2011) and observations (Hayes, 1979; FitzGerald, 1996).

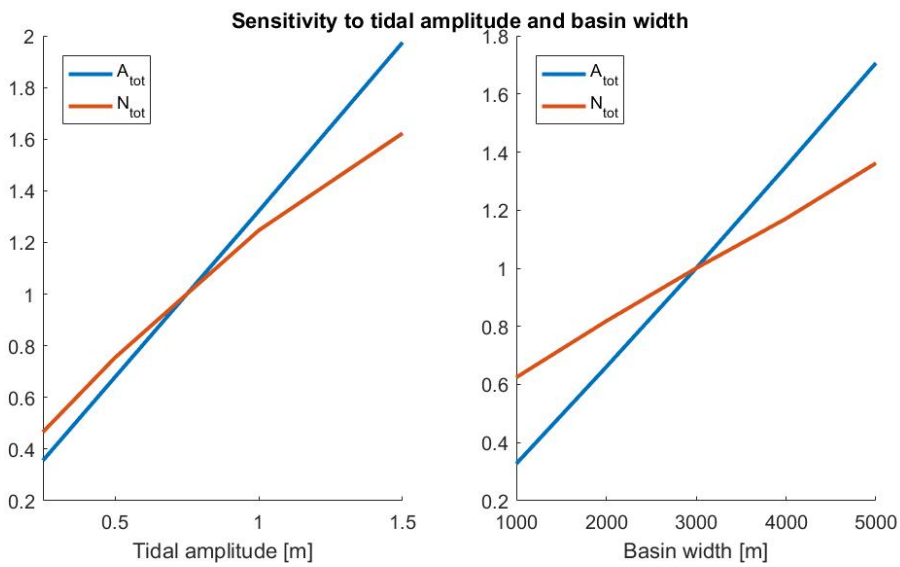

FIGURE 4.6: Sensitivity to tidal amplitude and basin width (relative to tidal amplitude of 0.75m and basin width of 3000m)

4.4 Predicting evolution of new inlet

The previous sections has focussed on the equilibrium state and maximum values of the system. This section describes the development of the system towards these equilibria and maxima. With this, connections are to be found so it can be predicted what the effects will be of a breach on the existing inlets and how it will develop itself. This prediction can be based on three variables: stage of the system, location of the breach and the initial width of the breach.

4.4.1 Three stages in time

In section 4.2.2 the average development of the system in time is divided in three stages. The difference between these stages can clearly be seen when analysing the decrease ratio.

Figure 4.7 shows with a cdf of 10,000 simulations the decrease ratio of the three stages: the green one of stage I, the blue one of stage II and red one of stage III. The decrease ratio is on the horizontal axis and the percentage of simulations that the decrease ratio was lower than a certain percentage on the vertical axis. The R_i differs between the stages with a higher value for the latter years (stage III) and a lower value for the first years (stage I). In 98% of all simulations, less than 60 percent of all breaches created in the first 150 years decreased in size the first time step after opening. Even in 20 percent of the simulations, less than one of seven inlets immediately decreased in size. Completely different results are shown in stage III. In none of the simulations, less than 70% of all breaches decreased in size directly after opening and in 88% of the simulations this was more than 90%. Stage II shows decrease ratios in between those of stage I and III with ratios varying between 50 and 100 percent.

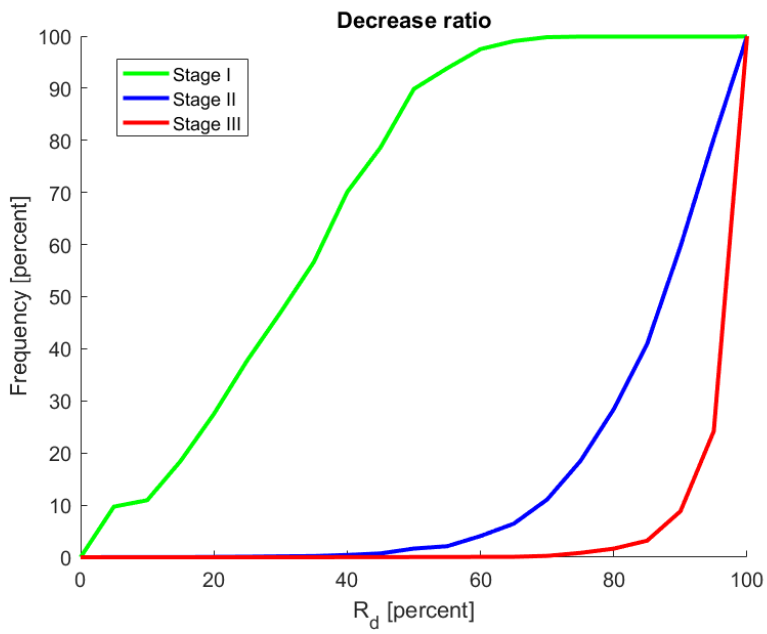

FIGURE 4.7: Percentage of inlets that initially decreased in size, per stage

4.4.2 Distance to closest neighbouring inlet

A second property of a breach that explains part of the tendency of a new inlet to close or stay open is the location of the breach and specifically the distance between the new inlet and the closest neighbouring inlet (D_j). This property is dominant over the initial inlet width, see Figure A.5 in Appendix A. Small existing inlets (smaller than 2 times the breach width) are filtered out when determining this distance as the small and closing inlets have at most a minor effect on the development on new inlets.

The distance of a new inlet to its neighbouring inlet relative to the length of the basin is plotted against the decrease ratio in Figure 4.8. The figure shows that all inlets with D_j higher than 20% of the basin width (or 17.500 metres), initially increased in size. For the distances under 20% of the basin width a clear dependency of R_d on D_j is shown. For inlets close to an existing one R_d is 99% and this percentage strongly decreases to 0% as the distance between neighbouring inlets increases.

This result is clearly related to the three stages of tidal inlet system development as mentioned before. When splitting the results into the three stages it can be seen that the course of the three graphs are similar to each other and the aggregated graph in Figure 4.7. This shows that independent of the stage, the decrease ratio decreases with increasing distance between inlets. The difference between the stages is that the decrease ratio for stage I is lower than for the other stages and the decrease ratio for stage III slightly higher than for the other stages. These results per stage can be found in Appendix A, Figure A.7.

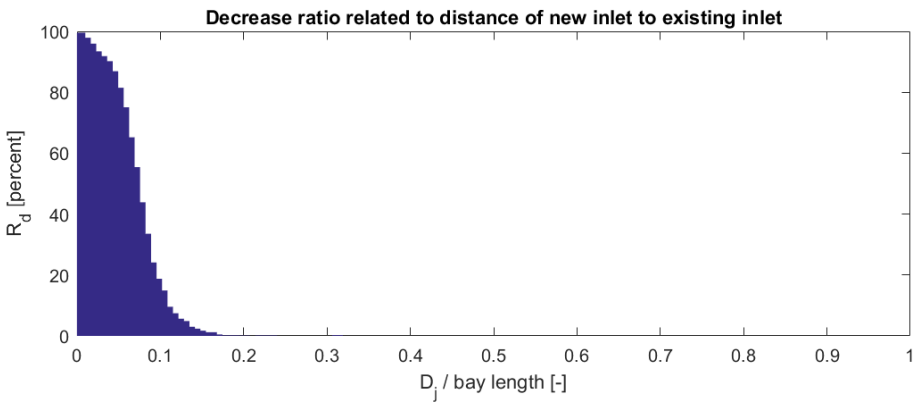

FIGURE 4.8: Decrease ratio of inlets opening within a certain distance from an existing inlet

4.4.3 Breach width

The other relation that determines the evolution of a breach, is the width of the breach. All inlets of the Monte Carlo simulation are plotted in Figure 4.9 based on their initial width and their lifetime. The colour of the dots indicate whether the inlet initially increased or decreased in size. The figure shows three results. First of all, a trend line is plotted (the dotted line in the figure). This trend lines shows that the wider the inlet is at the moment of breaching, the longer the lifetime of that inlet is. Small breaches can close within a year while bigger breaches take decades to close. The trend lines suggests a quadratic dependency. The second result is the difference between the two colours of dots. The inlets that decrease in size in the first time step after breaching close much quicker than those that increased in size. Especially for inlets smaller than 150 metres, a difference between the two groups is visible. The decreasing inlets do all, with just a few exceptions, close quickly (within years or a few decades) while the lifetime of increasing inlets is much more spread out. The third result visible in the figure is the red line showing the decrease ratio for inlet widths up to 150. The ratio decreases for increasing width. This means that the bigger the breach, the higher the chance the inlet will grow and stay open. This holds for all three stages as clarified in Figure A.8 in Appendix A. the dependency of the decrease ratio on initial breach width is stronger for breaches in stage I. The decrease

ratio is not plotted for breaches wider than 150 metres because those breaches might be wider than the equilibrium width of an inlet and the definition of opening and closing based on the first time step is then not applicable.

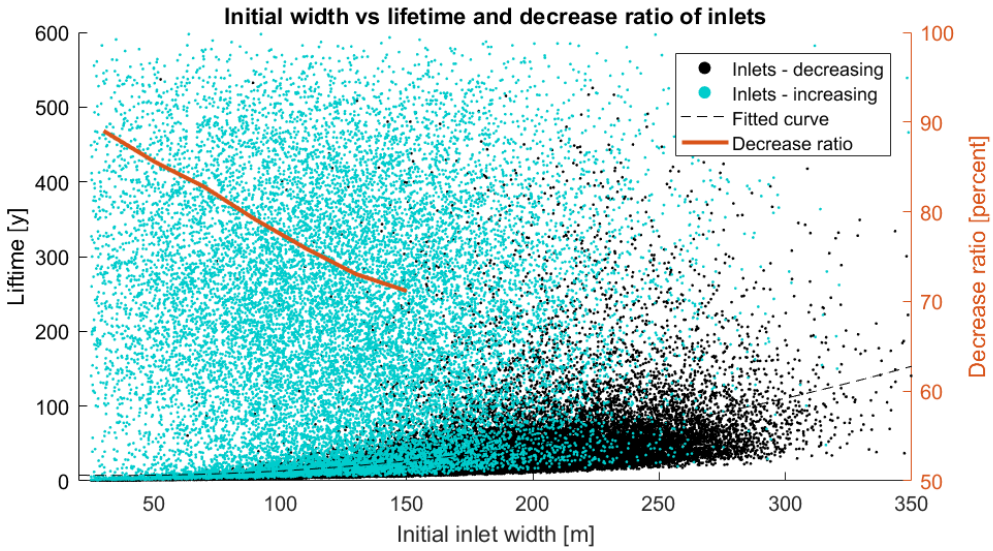

FIGURE 4.9: Lifetime and decrease ratio of inlets plotted against width of the breach, with colour of the dots indicating initial evolution of the inlet

4.5 Sensitivity

The section start with a sensitivity analysis which is performed for the implemented breach parameters: breach width and breach frequency. Next the effects of an addition to the model is elaborated: the widening of existing inlets during storms. These sensitivity analyses help to find the most important parameters and to study the effect of choices in input on the results. Besides, the sensitivity analysis can be used as an indicator of the consequences of climate change. According to Christensen et al. (2013), there is a likely increase in global mean tropical cyclone maximum wind speed. However, the influence of climate change on tropical cyclones is likely to vary by region and there is low confidence in region-specific projections of frequency and intensity of cyclones. Thus, no specific values can be used in the model to simulate climate changes. The possible changes in climate can now be studied by (1) extending the study of the effect of storms by including widening of inlets during storms and (2) varying the storm and breach frequencies, the breach width and the widening of inlets to study the effect of possible storm frequency and intensity increases.

4.5.1 Sensitivity of breach width and breach frequency

Two important parameters that are used in the model, are the breach frequency and the mean breach width. The effect of varying these input parameters on total inlet area (A_{tot}) and number of open inlets (N_{tot}) is found. But also, the effect of varying the input on the characteristics of the new inlets is searched for. Specifically the lifetime of the inlets (L_j).

The equilibrium values of the system (both (A_{tot}) and (N_{tot})) is found to be insensitive to the frequency of breaching (f_b). The same holds for the mean life time. The sensitivity graph can be found in Figure A.9 in Appendix A. When zooming in on these results, the effect of breach frequency can be found: changing the f_b affects the moment the equilibrium state is reached. This can be seen in Figure 4.10. For different values of f_b, A_{tot} over time is plotted. The higher f_by, the earlier the equilibrium state is reached. Also, the overshoot in f_b just before equilibrium is reached, is more clear when f_b increases. This is the result of the fact mentioned earlier, that the time scale of growing into a stable inlet is smaller than for existing inlets to decrease in size. When f_b is higher, this system has on average less time to adapt to a new inlet so higher inlet areas than equilibrium is more common. For the lowest values of f_b, the fact is not noticeable at all. The slight dependency of N_{tot} on the f_b is a result of the phenomenon mentioned above. The equilibrium value of the number of open inlets is reached later in time. The mean number of open inlets over the last 200 years will thus be slightly lower.

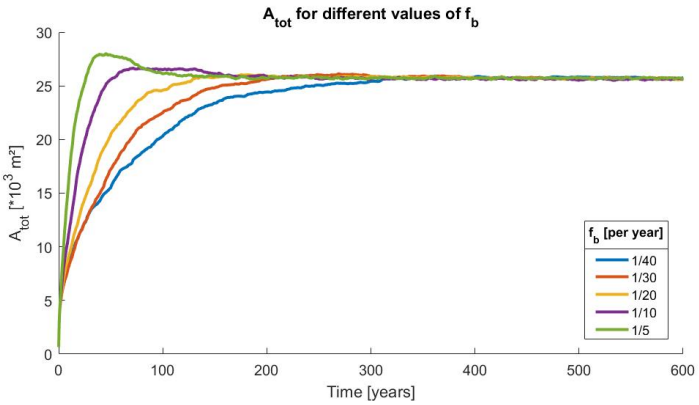

FIGURE 4.10: Sensitivity of evolution of total inlet area in time to breach frequency

The sensitivity of the system to the mean breach width (b_b)is shown in Figure 4.11. There is hardly dependency between b_b and the equilibrium state of the system. However, the breach width clearly affects the lifetime of inlets. The higher b_b are, high L_j.

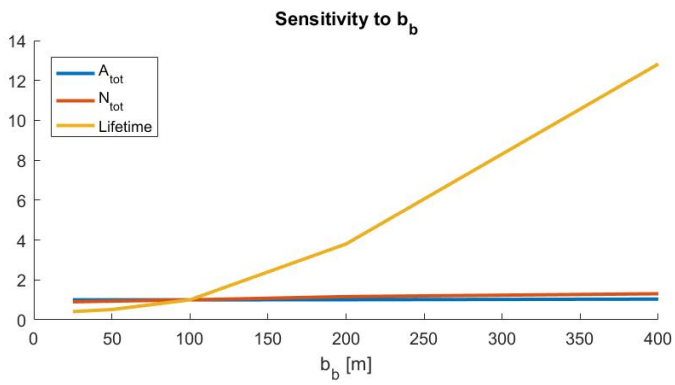

FIGURE 4.11: Sensitivity (relative to breach width of 100m) to mean breach width

4.5.2 Widening of inlets during storms

As mentioned in Chapter 2, barrier island breaching is a phenomenon that occurs during storms. But besides breaching there is an other observed effect of storms: existing inlets widen because of the water level set up and high wind speeds. Therefore, widening of existing inlets as a result of a severe storm can as an extra stochastic element be included in the model. The results for including the widening of inlets is presented for different values of the input parameters of this stochastic process namely the occurrence of storms and the widening factor of the inlets.

In the model we assume that when the tidal range increases during a storm, the flow velocity in every inlet increases with an equal amount. Therefore, according to Escoffier, the increase in cross sectional area is the same for every inlet. A multiplication factor (M) is used to calculate the total inlet area after the storm passed. The increase in A_{tot} is then divided by N_{tot} to know the increase in area per inlet. For this sensitivity analysis, runs are performed for values of M ranging between 1 and 1.5 with 1 being the standard situation without inlet widening. A_{tot} is restricted to a maximum that is determined by calculating A_{tot} using the maximum tidal range (being 2.12 metres (Meteo365, 2017)) that was observed in the study area in the past. Coastal storms that cause severe damage have a recurrence interval of 5 years (or a frequency f_s of 1/5 per year) in New York, according to Mather et al. (1964). For the sensitivity analysis, values for f_s of 1/3, 1/5, 1/10 and 1/20 years are used. In the model, the probability distribution of breach occurrence is coupled to the one of storm occurrence, so a breach could only take place when there is a storm. The effect of including widening of inlets during storms, is shown in Figure 4.12 and Figure 4.13. An example run can be found in Appendix A, Figure A.10.

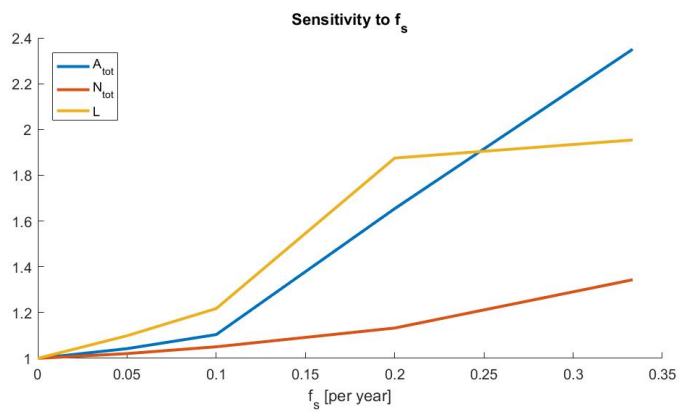

FIGURE 4.12: Sensitivity to storm frequency (relative to a f_s=0) with M=1.1

The first effect of including widening of inlets during storms, is the increase in total inlet area. Figure 4.12 shows A_{tot} for different values of f_s and Figure 4.13 shows the evolution of A_{tot} in time for different values of M. Both figures show a similar result: the higher the storm frequency the higher the total area, and also the higher the multiplication factor of the total inlet area the higher the total area. For low values of f_s and M, A_{tot} is increased only for a short period because the system returns to its equilibrium state in a few years. But for higher values of f_s and M, there might not be enough time between two subsequent storms to restore the equilibrium. In this situation, A_{tot} is permanently bigger than the equilibrium value.

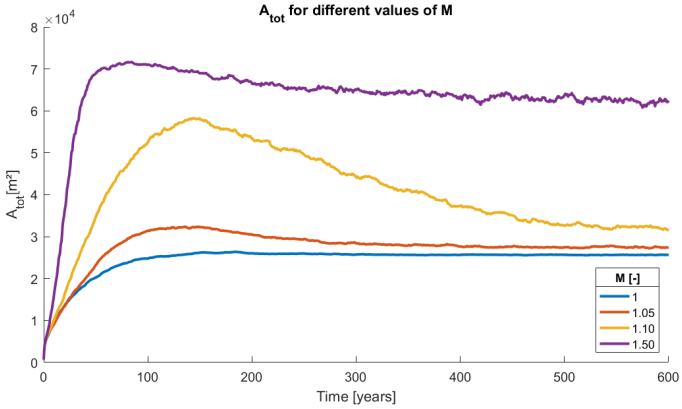

FIGURE 4.13: Sensitivity to M with f_s=1/5 per year

For f_s equal to 1/3 or M equal to 1.5, the effect is almost the same as for increasing the tidal range but with a more fluctuating inlet area.

A second effect of the inlet widening during storms is that the lifetime of inlets is longer, this is shown by the yellow graph in Figure 4.12. When a storm occurs, inlets that are almost closed get wider again and it therefore takes longer to close. In the extreme cases with high storm frequencies, some inlets do not close at all. This same effect is visible in the number of open inlets, this is a few higher when the breach frequency increases.

4.6 Subconclusion

When storm-induced breaches are included, some of the breaches close within a few years while others stay open longer up to hundreds of years. The system responds to the breaches by finding a new equilibrium state depending on whether the equilibrium total inlet area and maximum number of open inlets is reached. The total inlet area and number of open inlets correspond to the case without storm-induced breaches and are sensitive to input parameters such as breach frequency and breach width. Changes in storm climate as storm intensity and frequency increases lead to an increase in total inlet area.

Chapter 5

Discussion

This chapter discusses the methodology and the results as described in previous chapters. This consists of a review of used data en assumptions and a reflection of the results.

5.1 Link between storm and breach

In this study we start modelling from the moment a breach is created by a storm. The processes prior to this, so the the occurrence and properties of a breach in relation to the properties of the storm, are found by relating the Beaufort Force of a storm to the size of a breach. This method is chosen because of a lack of data. The results give an indication of which type of storms can cause breaches. However, it is favourable to use a less simplistic method. Since breaching is a local phenomenon, it should include factors such as direction of the wind and local height of the dune.

Because there is no relation known between storm properties and breaches, the probability distributions that are included to simulate storm-induced breaches, are based on historical observations of breaches. Also in the documented breach area, the lack of data leads to uncertainty. Often no information is provided on the way of measuring the breach area though it does influence the outcome of the measurement. A few examples are the moment of measuring (during high or low tide), the date of measuring (1 day or month after the storm) and the location of measuring (at the deepest and widest point, or averaged over the entire inlet). The consequence is that the breach areas do give an indication of the range of breach areas but they might not be completely comparable to each other. The probability distributions in the model are based on the historical data of breach size and as demonstrated in the sensitivity analysis, changes herein affect the quantitative results of the simulation.

5.2 Model assumptions and simplifications

In this study, an idealized model has been used. This model type is most suitable to simulate long term evolution and is generic so it can easily be applied to other study areas. However, it should be kept in mind that simplifications have been made in both the general model set up and the breach inclusion and that the input parameters are based on estimations. Because of this, the results explain only the very general behaviour of the system.

In the general model set up, the most important simplification is the simple and straight geometry of inlets and basin. Flow patterns might differ for geometries that are not rectangular shaped which would result in a different configuration of the locations and number of open inlets. Also, migration of inlets is not possible in the

model while observations show this phenomenon often. We also neglect other natural phenomena as variations in grain size, inlet migration and the presence of inlet deltas and shoals. In breaching parameters, simplifications have been made in the location of the breach which is now assumed to be uniformly distributed. Previous studies however show dependency on the topography of the islands. Also, the number of breaches and breach size are determined with probability distributions based on breach events in the past. They are now treated separately, while they both depend on storm frequency. So the model does not completely match with reality where the number of breaches and the breach size might be coupled. The input parameters that are used are based on available data and estimations. The sensitivity analysis shows clear dependency of the results on the value of the input. Especially on tidal range and basin area but also on breach parameters. Small changes in input might thus lead to different results in inlet area and number of open inlets.

Because of the simplifications and the sensitivity of the estimated input parameters, the results should be interpreted qualitatively over quantitatively. The exact values of the output might differ in reality but the results give a good representation of the qualitative development of the system. The results of this study could therefore be used by policy makers for prevention of breaches and by decision making after a breach have occurred. Based on these results a quick initial guess could be made what the development of the breach and the other inlets will be and based on this, it can be decided if and how soon measures should be taken. The results can not be used to get to know the exact dimensions and locations of inlets in a tidal inlet system.

5.3 Results

To evaluate the development of a breach a definition is based on the first time step after opening. We assume that the initial change in cross sectional area continues until the inlet is either closed or has found its equilibrium width. Thus, inlets that decrease in size in the first time step are expected to close, inlets that increase are expected to stay open. Inlets of the latter group might close eventually ass well, but this will mostly be an external effect as a new inlet has opened that competes with the old ones. It could, however, also be, that the inlets development changes after the first time step or that inlets are wider during the breach than they will be in equilibrium. In these cases the current definition of development of the inlet is not correct. For breaches smaller than 150 metres wide, the definition is expected to be applicable as more than 99% of the inlets marked as decreasing in size closed within 30 years. For bigger breaches it is not certain to be applicable as many inlets that decreased in size did stay open for up to 600 years and only 77% of the inlets marked as decreasing in size closed within 30 years.

The results of this study meet the expectations as they are in line with observations and earlier studies. When a breach occurs, sometimes the effect is little and the breach closes in several years. But sometimes the entire system is affected as some current inlets decrease in size or even keep filling up until closure. This is in line with observations as presented in Chapter 2 and also as suggested by (Wang and Roberts Briggs, 2015). The system evolves onto an equilibrium in total inlet area as is observed in many systems (Escoffier, 1977; Van De Kreeke et al., 2008) and has a maximum number of inlets that can be open which is in line with Roos et al. (2013). The value of this equilibrium and maximum states are dependent on the input parameters. With an increased tidal range or bigger basin area, more inlets can be open

and the total inlet area is higher. This is in line with the study of (Stutz and Pilkey, 2011). An important factor wherein the model differs from reality is that the model only includes natural effects while human interventions are common in reality. Including human interventions might chance the development of the system.

Chapter 6

Conclusions and recommendations

This study presents the long term modelling of multiple tidal inlet systems including barrier island breaching during storms. This final chapter provides answers to the three research questions as stated in chapter 1 and draws conclusions. The last section denotes recommendations for further research that follow from this study.

6.1 Conclusions

6.1.1 Under what conditions do barrier islands breach, what are the spatial characteristics of the breaches and how do they develop?

Barrier island breaching is a phenomenon that has occurred multiple times in history. Many of these breach events are not well documented and little data is available. Observations of past breach events are used as data source. What can be learned from observations is the following. Storms cause besides breaching also widening of existing inlets. Breaching can occur both from basin and from sea side during storms of at least Beaufort Force 10. Depending on the storm characteristics and the topography of the tidal inlet system, water level set up and high wind speeds can then be the cause of inundation. Water flows over the island and carves a channel: a breach is created. Multiple breaches on different locations can occur and the area of these breaches range between 20 and 600 squared metres. Some of the breaches close naturally within a few months, others grow in size and become permanent inlets. In the latter case, the entire system is affected and existing inlets might decrease in size or close. Because the fear of people for flood and navigation problems, breaches are often artificially closed, fixed with jetties or dredged.

6.1.2 How can storm-induced breaches be described in a stochastic way and implemented in the idealized model of Roos et al. (2013)?

Including barrier island breaching in the idealized deterministic model is done by introducing three probability distributions. Every time step in the simulation there is, based on these distributions, randomly decided if a breach occurs and what properties the breach has. The first distribution is used for the occurrence and number of breaches with chances based on historical breach events. The second distribution is uniform and is used for the location of the breach. The third distribution is an adjusted normal distribution that is used for the size of the breach with a range based on historical data. The stochastic input requires a statistical approach when analysing the results. A Monte Carlo simulation is performed resulting in statistical details of the systems response to the breach events.

6.1.3 How does the model (as set up in research question 2) respond to the stochastically created breaches and can the inlet stability concept be expressed in a dynamical way?

What is the effect of storm-induced breaches on the development and equilibrium state of a tidal inlet system?

Similar to the model without storm-induced breaches of Roos et al. (2013), the system evolves towards an equilibrium state. In this equilibrium state the sum of the cross sectional area of all inlets remains the same. Introducing a breach disturbs this equilibrium because of the addition of inlet area. Either the new inlet will close or existing ones will decrease in size or close to restore the equilibrium in inlet area.

The equilibrium state of the system and the time it takes to reach this state depends on the input parameters. The system is especially sensitive to the tidal range and basin area as increasing one of these increases the total inlet area and maximum number of open inlets. The moment an equilibrium is reached depends on the breach frequency and size. Introducing side effects of storms as widening of existing inlets changes the evolution of new inlets and the entire system. The lifetime of inlets increases up to a factor two depending on the storm frequency and the system will deviate from its equilibrium state as the total inlet area and number of open inlets increase during a storm and it takes a few years to recover.

What are the most important factors that determine the development of new inlets?

The development of a breach depends mainly on three factors: the state of the system, the distance of the breach to existing inlets and the width of the breach. The state of the system can be divided in three stages with descending chance that an inlet will stay open. The first is when no equilibrium has been reached by the system. The majority of the breaches in this stage become a permanent inlet. Existing inlets might be unaffected. In the second stage the system has reached the equilibrium state of total inlet area. The majority of the breaches close but some stay open causing existing inlets to decrease in size. In the third stage, the system consists of the maximum number of inlets. More than 90% of the breaches close and in the cases that new inlets do stay open one of the existing inlets will close.

The second factor that explains the tendency of a breach to stay open or not is the distance of the breach to the nearest open inlet. The larger this distance, the higher the chance an inlet will stay open. For distances larger than 20% of the basin width, all breaches grew in size and the inlet stayed open while the for very small distance almost every inlet closed.

The last factor is the initial width of the inlet. Bigger inlets stay open longer and have a lower chance to decrease in size after opening. The latter holds for breaches smaller than the equilibrium size of an inlet (or 150 metres wide) only.

6.2 Recommendations

The results show that based on the location and width of a breach an estimation can be made how the breach and the other inlets of the system will develop. This estimation can be used in barrier coast management to decide whether it is necessary to interfere in the system right after a breach occurs. It is recommended to extend and specify this research subject to improve the certainty of the estimation what will happen in the system. The following recommendations contribute to that.

More research should be directed towards the quantitative relation between a storm and a breach. This should include the most important storm parameters as

wind speed and direction and the most important topographical properties as height and width of the island. This way, a more accurate probability distribution of breach occurrence can be introduced which can then be coupled to the cross sectional area of the breach. Improving the relation between storms and breaches will be very beneficial to the ability to predict breaches.

This study only explains the general behaviour of the system and breaches. To be able to predict the development of a specific study area better, it is recommend to choose input that suits better with the study area. Examples are a non-rectangular geometry of the basin, varying depth in basin and inlets and a varying tidal range along the coast.

Lastly, it is recommend to further include some extra effects that play an important role in reality. First of all by extending the effect of storms by not only allowing breaches but by also including the widening of inlets during a storm. Besides, changes in climate, as increased storminess and increased sea level, should be implemented in the model because of the long time span. Also including the impact of human interventions should be considered. The current model is only based on natural effects but dredging, artificially closing and fixing inlets by jetties are human interventions that change the natural behaviour of the system.

Bibliography

Blake, E. S., T. B. Kimberlain, R. J. Berg, Cangia, J. P. Losi and J. L. Beven II (2013). *Tropical cyclone report - Hurricane Sandy*. Tech. rep. National Hurricane Center. DOI: 10.1017/CBO9781107415324.004.

Brouwer, R., J. Van De Kreeke and H. Schuttelaars (2012). 'Entrance/exit losses and cross-sectional stability of double inlet systems'. In: *Estuarine, Coastal and Shelf Science* 107, pp. 69–80. ISSN: 02727714.

Brouwer, R., H. M. Schuttelaars and P. C. Roos (2013). 'Modelling the influence of spatially varying hydrodynamics on the cross-sectional stability of double inlet systems'. In: *Ocean Dynamics* 63.11-12, pp. 1263–1278. ISSN: 16167341.

Cañizares, R. and J. L. Irish (2008). 'Simulation of storm-induced barrier island morphodynamics and flooding'. In: *Coastal Engineering* 55.12, pp. 1089–1101. ISSN: 03783839. DOI: 10.1016/j.coastaleng.2008.04.006.

Christensen, J., K. K. Kumar, E. Aldria, S.-I. An, I. Cavalcanti, M. D. Castro, W. Dong, P. Goswami, A. Hall, J. Kanyanga, A. Kitoh, J. Kossin, N.-C. Lau, J. Renwick, D. Stephenson, S.-P. Xie and T. Zhou (2013). 'Climate Phenomena and their Relevance for Future Regional Climate Change Supplementary Material'. In: *Climate Change 2013: The Physical Science Basis. Contribution of Working Group I to the Fifth Assessment Report of the Intergovernmental Panel on Climate Change*, p. 62. ISSN: 0148-0227. DOI: 10.1017/CBO9781107415324.028. URL: www.climatechange2013.org.

Clinch, A. S., E. R. Russ, R. C. Oliver, H. Mitasova and M. F. Overton (2012). 'Hurricane Irene and the Pea Island Breach: pre-storm Site Characterization and Storm Surge Estimation Using Geospatial Technologies'. In: *Shore and Beach* 80.2, pp. 38–46.

De Swart, H. E. and N. D. Volp (2012). 'Effects of hypsometry on the morphodynamic stability of single and multiple tidal inlet systems'. In: *Journal of Sea Research* 74, pp. 35–44. ISSN: 13851101. DOI: 10.1016/j.seares.2012.05.008.

De Swart, H. and J. Zimmerman (2009). 'Morphodynamics of Tidal Inlet Systems'. In: *Annual Review of Fluid Mechanics* 41.1, pp. 203–229. ISSN: 0066-4189. DOI: 10.1146/annurev.fluid.010908.165159.

Escoffier, F. F. (1940). 'The stability of tidal inlets'. In: *Shore and Beach* 8.4, pp. 114–115.

Escoffier, F. F. (1977). *Hydraulics and Stability of Tidal Inlets*. Tech. rep.

FEMA (2013). 'Mitigation Assessment Team Report: Hurricane Sandy in New Jersey and New York. Building Performance Observations, Recommendations, and Technical Guidance'. In: FEMA P-942, p. 223.

Fenton, G. A. and D. V. Griffiths (2008). *Risk Assessment in Geotechnical Engineering*. Hoboken: John Wiley & Sons, Inc., p. 463. ISBN: 9780470178201.

FitzGerald, D. M. (1996). 'Geomorphic Variability and Morphologic and Sedimentologic Controls on Tidal Inlets'. In: *Journal of Coastal Research* 23, pp. 47–71. ISSN: 07490208. DOI: 10.2307/25736068. URL: http://www.jstor.org/stable/25736068.

Flagg, C. (2012). *Initial Report for the Evaluation of Wilderness Breach , Fire Island National Seashore*. Tech. rep.

Flagg, C. (2013). *The Development of the Old Inlet Breach and its Impact on Great South Bay*. URL: https://www.youtube.com/watch?v=yCI0ryDUUMI.

Flagg, C., C. Hinrichs, R. Flood and R. Wilson (2016). *Update on the Status of Old Inlet Breach*. Tech. rep.

Flagg, C., R. E. Wilson, C. Hinrichs and T. Wilson (2017). *The Great South Bay Project*. URL: http://po.msrc.sunysb.edu/GSB/.

Foderaro, L. W. (2016). *On Fire Island, a Scar From Hurricane Sandy Is Now Seen as a Good Thing*. New York. URL: https://www.nytimes.com/2016/10/04/nyregion/on-fire-island-a-scar-from-hurricane-sandy-is-seen-as-a-good-thing.html?_r=0.

Friedrichs, C. T., D. G. Aubrey, G. S. Giese and P. E. Speer (1993). 'Hydrodynamical Modeling of a Multiple-Inlet Estuary/Barrier System: Insight Into Tidal Inlet Formation and Stability'. In: *Coastal and Estuarine Studies* 44, pp. 95–112. ISSN: 0875902588. DOI: 10.1029/CE044p0095.

Google Inc. (2017). *Google Earth*.

Hayes, M. O. (1979). 'Barrier island morphology as a function of tidal and wave regime'. In: *Barrier Islands*. Ed. by S. Leatherman. Chap. 1, pp. 1–27. DOI: 10.1016/j.margeo.2017.02.016.

Hurricane Research Division (2017). *Tropical Cyclone Records*. URL: http://www.aoml.noaa.gov/hrd/tcfaq/E11.html.

Kraus, N. C., A Militello and G Todoroff (2002). 'Barrier Breaching Processes and Barrier Spit Breach, Stone Lagoon, California'. In: *Shore and Beach* 70.4, pp. 21–28. ISSN: 0037-4237.

Lerche, I. and B. S. Mudford (2005). 'How Many Monte Carlo Simulations Does one Need to do ?' In: *Energy exploration & exploitation* 23.6, pp. 405–427.

MacIvor, L. H. (1998). *Impacts to Piping Plover and Seabeach Amaranth from Long-Term Sand Management Component*.

Mallinson, D. J., S. J. Culver, S. R. Riggs, J. P. Walsh, D. Ames and C. W. Smith (2008). 'Past, present and future inlets of the Outer Banks barrier islands, North Carolina'. In: *East Carolina University Printing Press*. DOI: 2016-8-31.

Mandia, S. A. (2017). *Geological Impact of the 1938 Hurricane*. URL: http://www2.sunysuffolk.edu/mandias/38hurricane/geological_impact.html.

Mather, J. R., H. Adams and G. a. Yoshioka (1964). *Coastal Storms of the Eastern United States*. DOI: 10.1175/1520-0450(1964)003<0693:CSOTEU>2.0.CO;2.

Matias, A, O Ferreira and J. M. Alveirinho-Dias (1999). 'Preliminary results of the Cacela Peninsula (southern Portugal) replenishment'. In: *Boletin - Instituto Espanol de Oceanografia* 15, pp. 283–288. ISSN: 00740195 (ISSN).

Meteo365 (2017). *tide-forcast*. URL: https://www.tide-forecast.com/locations/Fire-Island-Breakwater-Long-Island-New-York/tides/latest.

Nahon, A., X. Bertin, A. B. Fortunato and A. Oliveira (2012). 'Process-based 2DH morphodynamic modeling of tidal inlets: A comparison with empirical classifications and theories'. In: *Marine Geology* 291-294, pp. 1–11. ISSN: 00253227. DOI: 10.1016/j.margeo.2011.10.001.

Oertel, G. F. (1985). 'The barrier island system'. In: *Marine Geology* 63.1-4, pp. 1–18. ISSN: 00253227. DOI: 10.1016/0025-3227(85)90077-5.

Roos, P. C., H. M. Schuttelaars and R. Brouwer (2013). 'Observations of barrier island length explained using an exploratory morphodynamic model'. In: *Geophysical Research Letters* 40, pp. 4338–4343. ISSN: 00948276. DOI: 10.1002/grl.50843.

Safak, I., J. C. Warner and J. H. List (2016). 'Barrier island breach evolution: Alongshore transport and bay-ocean pressure gradient interactions'. In: *Journal of Geophysical Research: Oceans* 121, pp. 8720–8730. DOI: 10.1002/2016JC012029. Received.

Sallenger, A. H. (2000). 'Storm Impact Scale for Barrier Islands'. In: *Journal of Coastal Research* 16.3, pp. 890–895.

Salles, P., G. Voulgaris and D. G. Aubrey (2005). 'Contribution of nonlinear mechanisms in the persistence of multiple tidal inlet systems'. In: *Estuarine, Coastal and Shelf Science* 65.3, pp. 475–491. ISSN: 02727714. DOI: 10.1016/j.ecss.2005.06.018.

Schubel, J., T. Bell and H. Carter (1991). *The Great South Bay*. State University of New York Press, p. 107.

Stutz, M. L. and O. H. Pilkey (2005). 'The relative influence of humans on barrier islands: Humans versus geomorphology'. In: *Reviews in Engineering Geology* 16.12, pp. 137–147. ISSN: 0080-2018. DOI: 10.1130/2005.4016(12).

Stutz, M. L. and O. H. Pilkey (2011). 'Open-ocean barrier islands: Global influence of climatic, oceanographic, and depositional settings'. In: *Journal of Coastal Research* 27.2, pp. 207–222. ISSN: 0749-0208. DOI: 10.2112/09-1190.1.

Terchunianf, A. V. and C. Merkert (1995). 'Little Pikes Inlet, Westhampton, New York'. In: *Journal of Coastal Research* 11.3, pp. 697–703.

Tran, T. T., J. Van De Kreeke, M. J. F. Stive and D. J. R. Walstra (2012). 'Cross-sectional stability of tidal inlets: A comparison between numerical and empirical approaches'. In: *Coastal Engineering* 60.1, pp. 21–29. ISSN: 03783839. DOI: 10.1016/j.coastaleng.2011.08.005.

Tung, T. T., D.-J. R. Walstra, J. van de Graaff and M. J. F. Stive (2009). 'Morphological Modeling of Tidal Inlet Migration and Closure'. In: *Journal of Coastal Research* 2009.56, pp. 1080–1084. ISSN: 07490208. DOI: 10.2307/25737953.

U.S. Army Engineer District New York (1976). *Fire island Inlet to Montauk Point, New York beach erosion control and hurricane protection project*. Vol. 1. ISBN: 3663537137. DOI: 10.1016/0003-6870(73)90259-7.

U.S. Geological Survey (2009). *Coastal Change During Hurricane Isabel 2003*. Tech. rep.

Van De Kreeke, J. (1990). 'Can multiple tidal inlets be stable?' In: *Estuarine, Coastal and Shelf Science* 30.3, pp. 261–273. ISSN: 02727714. DOI: 10.1016/0272-7714(90)90051-R.

Van De Kreeke, J., R. Brouwer, T. J. Zitman and H. M. Schuttelaars (2008). 'The effect of a topographic high on the morphological stability of a two-inlet bay system'. In: *Coastal Engineering* 55.4, pp. 319–332. ISSN: 03783839. DOI: 10.1016/j.coastaleng.2007.11.010.

Vogel, M. J. and T. W. Kana (1984). 'Sedimentation patterns in a tidal inlet system Moriches Inlet, New York'. In: *Coastal Engineering Proceedings*. Houston. Chap. 201, pp. 3017–3033.

Wamsley, T. V., K. K. Hathaway and M. Wutkowski (2010). *Hatteras Breach, North Carolina*. Tech. rep. US Army Corps of Engineers, p. 23.

Wang, P. and T. M. Beck (2012). 'Morphodynamics of an anthropogenically altered dual-inlet system: John's Pass and Blind Pass, west-central Florida, USA'. In: *Marine Geology* 291-294, pp. 162–175. ISSN: 00253227. DOI: 10.1016/j.margeo.2011.06.001.

Wang, P. and T. Roberts Briggs (2015). 'Storm-Induced Morphology Changes along Barrier Islands and Poststorm Recovery'. In: *Coastal and Marine Hazards, Risks, and Disasters*. Ed. by J. F. Shroder, J. T. Ellis and D. J. Sherman. Boston: Elsevier.

Chap. 10, pp. 271–306. ISBN: 9780123965387. DOI: 10.1016/B978-0-12-396483-0.00010-8.

Appendix A

Complementary figures

FIGURE A.1: Evolution of Old Inlet first six years after breach, retrieved from Flagg et al. (2017)

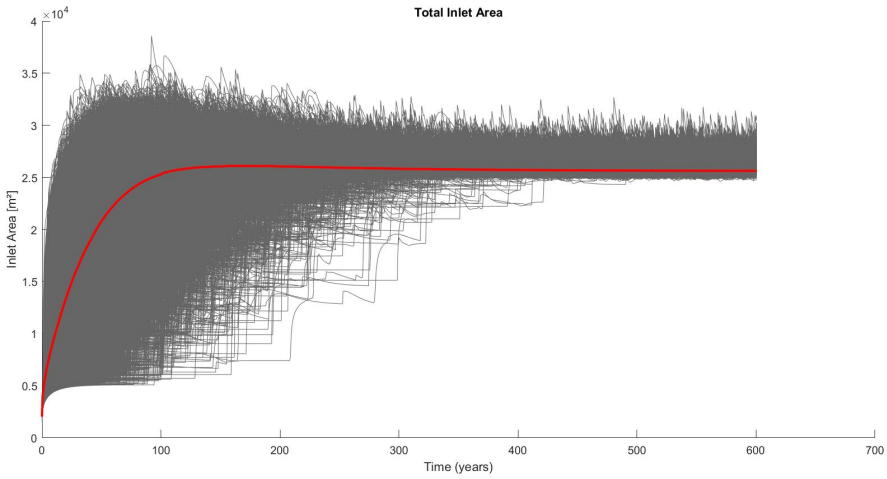

FIGURE A.2: Evolution of total inlet area in time for 10,000 simulations with red line showing the average

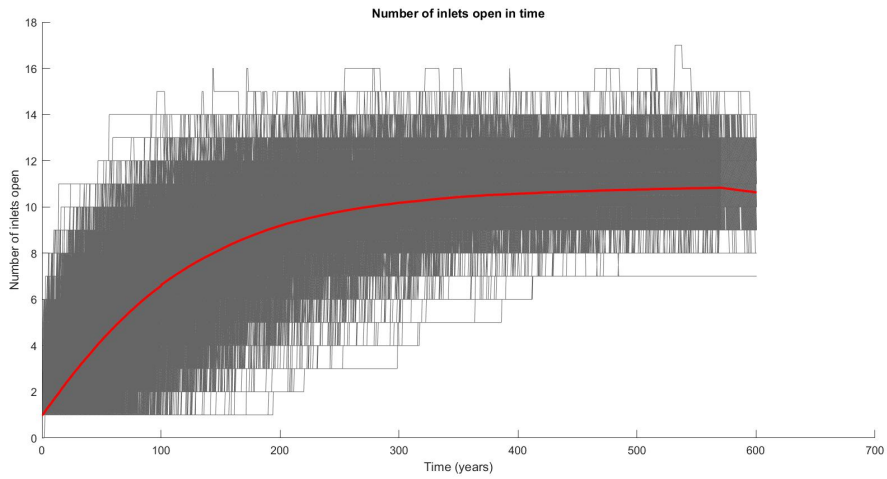

FIGURE A.3: Evolution of number op open inlets in time for 10,000 simulations with red line showing the average

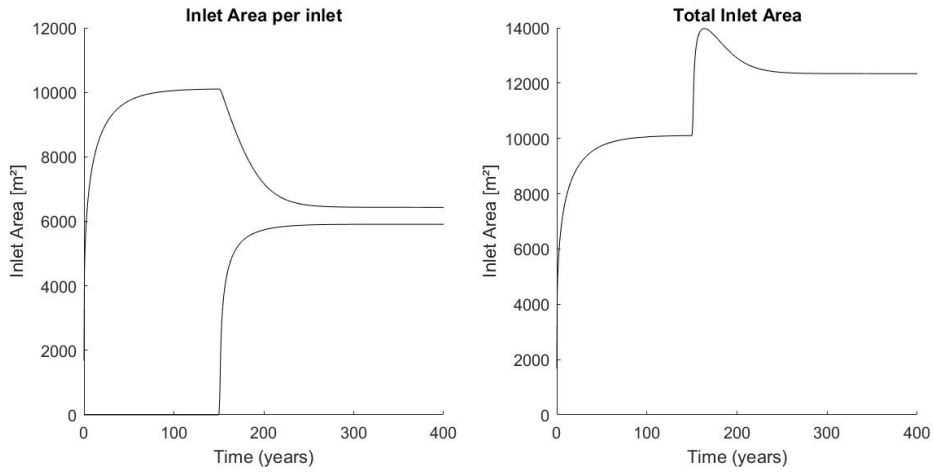

FIGURE A.4: Explanation of overshoot in inlet area. Increase in size is faster than decrease in size resulting in temporary high value of total area

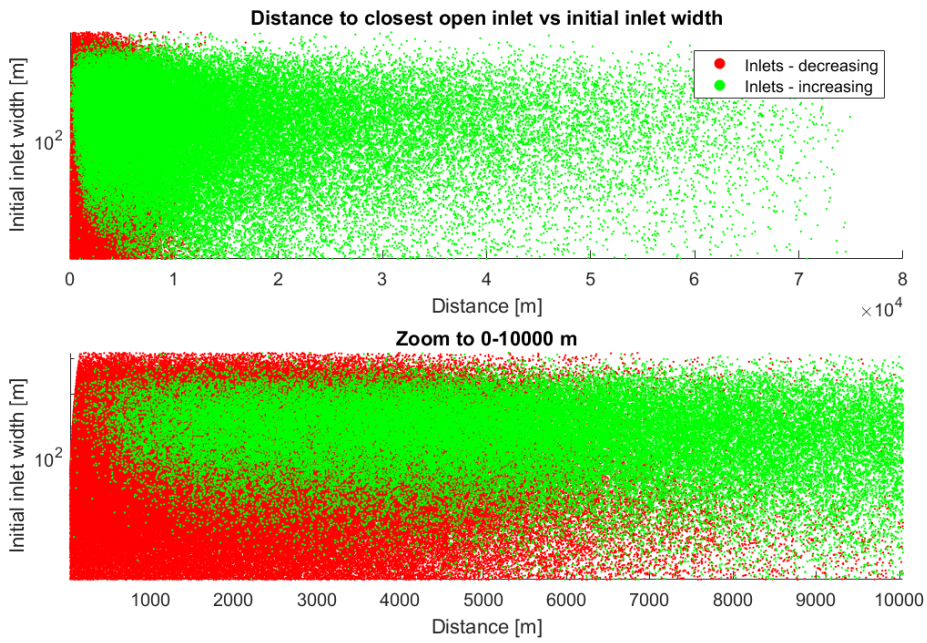

FIGURE A.5: Distance of a new inlet to its closest neighbour vs initial inlet width. With colour indicating the initial development of the inlet

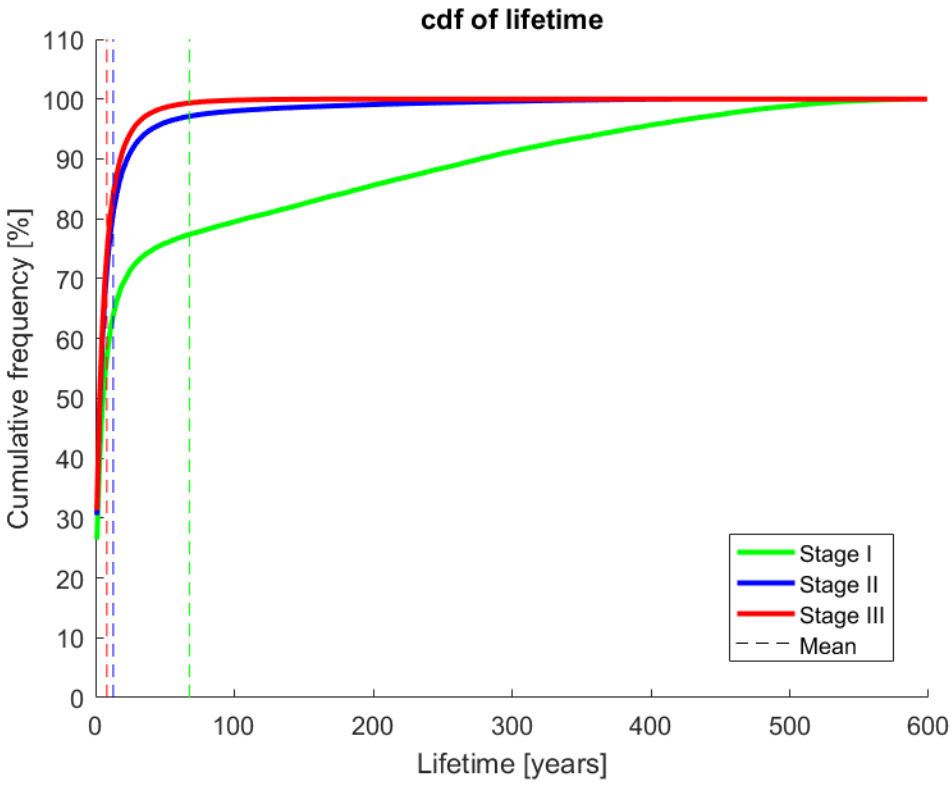

FIGURE A.6: Cumulative distribution of lifetime of inlets for sample run. Split into three stages

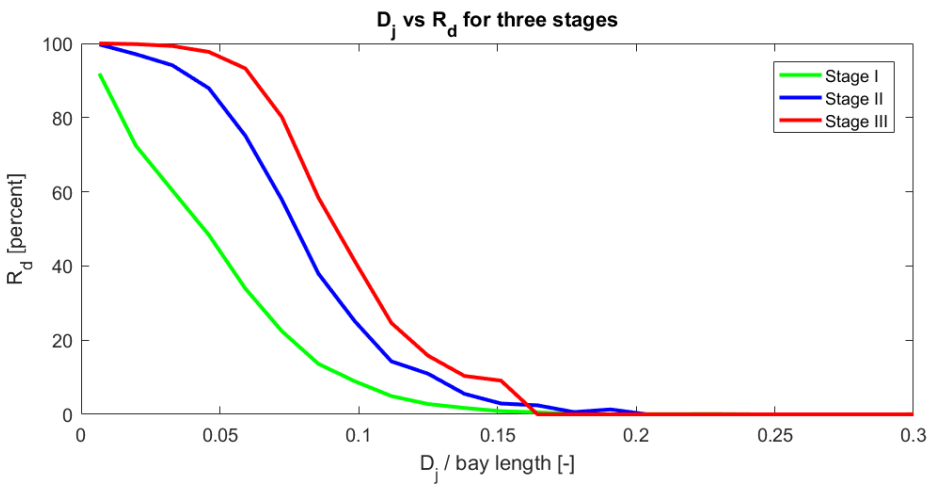

FIGURE A.7: Decrease ratio of inlets opening within a certain distance from an existing inlet. Split into three stages

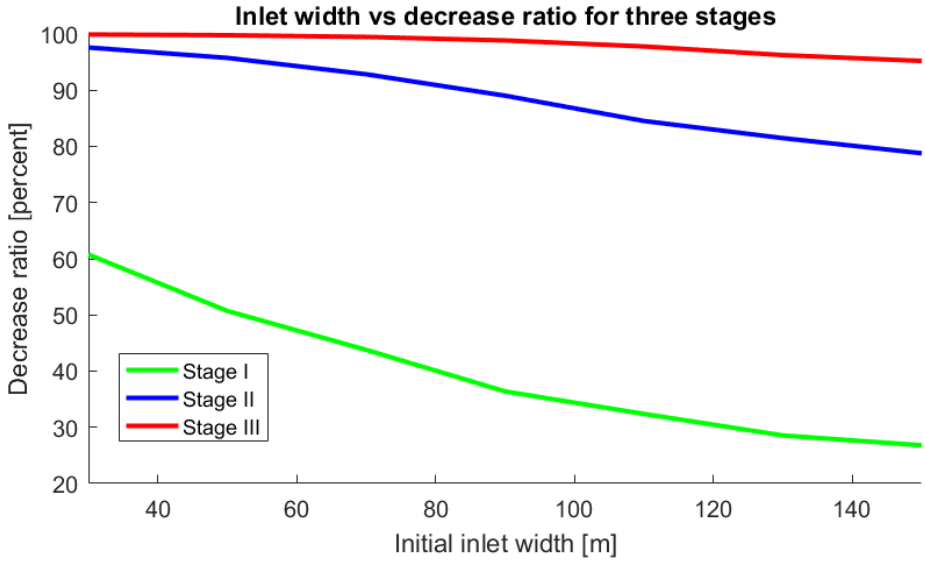

FIGURE A.8: Decrease ratio of inlets plotted against width of the breach. Split into three stages

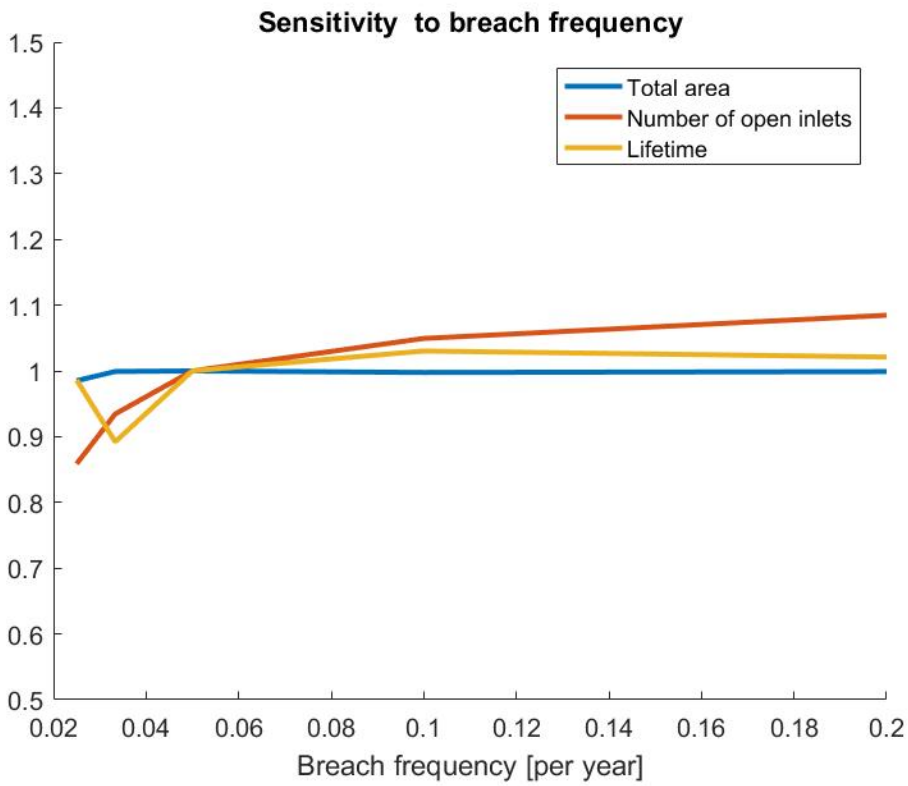

FIGURE A.9: Sensitivity of system to breach frequency, relative to a frequency of 1/20

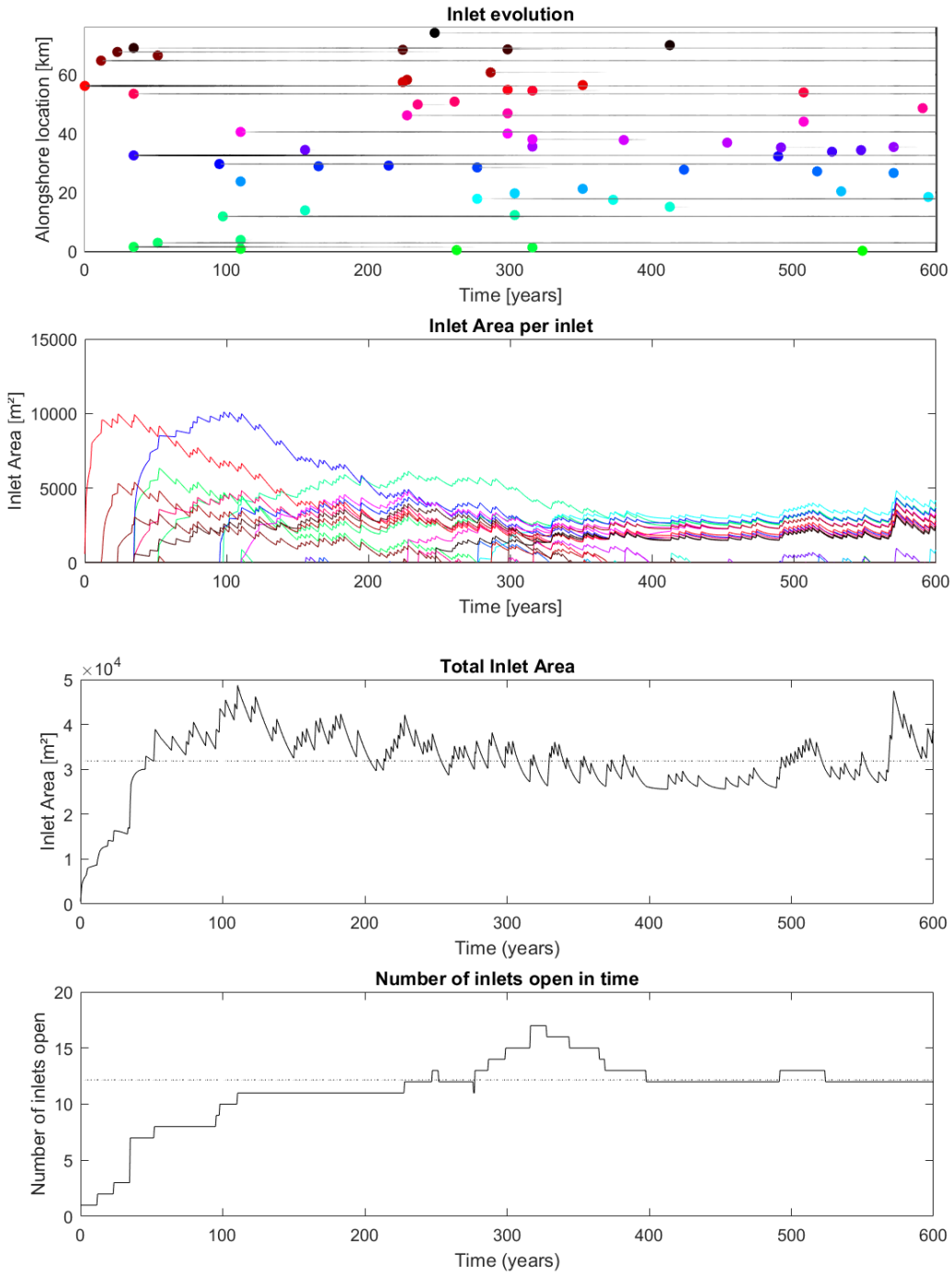

FIGURE A.10: Evolution of tidal inlet system when including widening of inlets during storms. With f_s=1/5 per year and M=1.1